The Digital Plateosaurus II: An Assessment of the Range of Motion of the Limbs and Vertebral Column and of Previous Reconstructions using a Digital Skeletal Mount

Author: Mallison, Heinrich

Source: Acta Palaeontologica Polonica, 55(3) : 433-458

Published By: Institute of Paleobiology, Polish Academy of Sciences

URL: https://doi.org/10.4202/app.2009.0075

The digital *Plateosaurus* II: An assessment of the range of motion of the limbs and vertebral column and of previous reconstructions using a digital skeletal mount

HEINRICH MALLISON

Mallison, H. 2010. The digital *Plateosaurus* II: An assessment of the range of motion of the limbs and vertebral column and of previous reconstructions using a digital skeletal mount. *Acta Palaeontologica Polonica* 55 (3): 433–458.

Scientific literature and museum exhibits are full of explicit and implicit claims about the possible postures and motion ranges of dinosaurs. For the example of the prosauropod *Plateosaurus engelhardti* I assessed the motion range of limbs and vertebral column in a CAD program using a 3D virtual skeletal mount. The range of motion of the forelimb is very limited, allowing the grasping of objects placed directly ventrally and ventrolaterally of the anterior torso. The manus is adapted for grasping. The powerful fore limb can barely reach in front of the shoulder, making a quadrupedal walking cycle impractical. Only a digitigrade pose of the pes with a steeply held metatarsus is feasible, and the morphology of the stylopodium and zeugopodium indicates a slightly flexed limb posture. Hind limb protraction and retraction are limited by the pelvic architecture. The neck has significant mobility both dorsoventrally and laterally, but blocks torsion. The dorsal vertebral column is flexible to a degree similar to the neck, mainly in the anterior half, but blocks torsion totally in the anterior and posterior thirds. The anterior dorsals are similar in shape to the posterior cervicals and significantly increase the motion range of the neck. The tail is highly flexible due to its large number of elements, showing more lateral than dorsoventral mobility. These results are compared to reconstruction drawings and museum skeletal mounts, highlighting a pattern of errors specific to certain widely used reconstruction methods.

Key words: Prosauropoda, *Plateosaurus*, reconstruction, digital skeleton, 3D model, accuracy.

Heinrich Mallison [heinrich.mallison@googlemail.com], Glambecker Weg 6, 13467 Berlin, Germany.

Received 26 May 2009, accepted 25 February 2010, available online 8 March 2010.

Introduction

Plateosaurus engelhardti Meyer, 1837 from the Upper Triassic of Central Europe is one of the best-known dinosaurs, with a large number of strikingly well-preserved skeletons found in Frick (Switzerland), Halberstadt and Trossingen (both Germany), and additional disarticulated finds from many other localities. *P. engelhardti* was also the fifth dinosaur to be described, and the first outside England (see Galton 2001). In addition to the holotype material, many skeletons were found in articulation in the first third of the 19th century, and the excavation of some of these was documented in detail, with figures published of the specimens as found in the ground (Jaekel 1913–1914; Huene 1926). One of the best finds of this kind, SMNS F33 from Trossingen, was prepared so that the association of all bones was retained, and remains in this state to this day (Fig. 1A). This specimen is the only one in which the anterior body does not rest on one side, but is upright (Sander 1992), offering insight into the articulation of the shoulder girdle difficult to gain from other specimens. Some other individuals, notably the most complete specimen ever found from Frick (MSF 23, Sander 1992), were also retained in articulation (Fig. 1B). On the basis of this huge amount of detailed data, one could assume that reconstructing the overall body shape, posture and locomotion of this animal is simple. To the contrary, the literature not only of the early 19th century, but even of recent years is full of contradictory reconstruction drawings and remarks on the locomotion of *Plateosaurus*. The history of biomechanical interpretations of the genus, the graphical representation of which will be discussed here, is nearly as complex and confusing as that of its taxonomy. Moser (2003) gives the latest detailed review, concluding that *Plateosaurus* is monospecific, with *P. engelhardti* as the sole species. However, Moser (2003) cautions that there is ample material labeled "*Plateosaurus*" in collections that does not belong to the genus. Yates (2003) assigns a second, more gracile and much rarer species, previously *Sellosaurus gracilis* Huene, 1907–1908, to *Plateosaurus* as *P. gracilis*. Here, "*Plateosaurus*" refers to the Halberstadt, Trossingen, Ellingen (Germany) and Frick material belonging to *P. engelhardti*.

The easiest way for a researcher to communicate his view of the body shape, locomotion and general appearance of an extinct animal is usually the creation of a reconstruction drawing. The tradition goes back to Marsh (e.g., *Triceratops* and "*Brontosaurus*" in Marsh 1891), and in recent years, in-

doi:10.4202/app.2009.0075

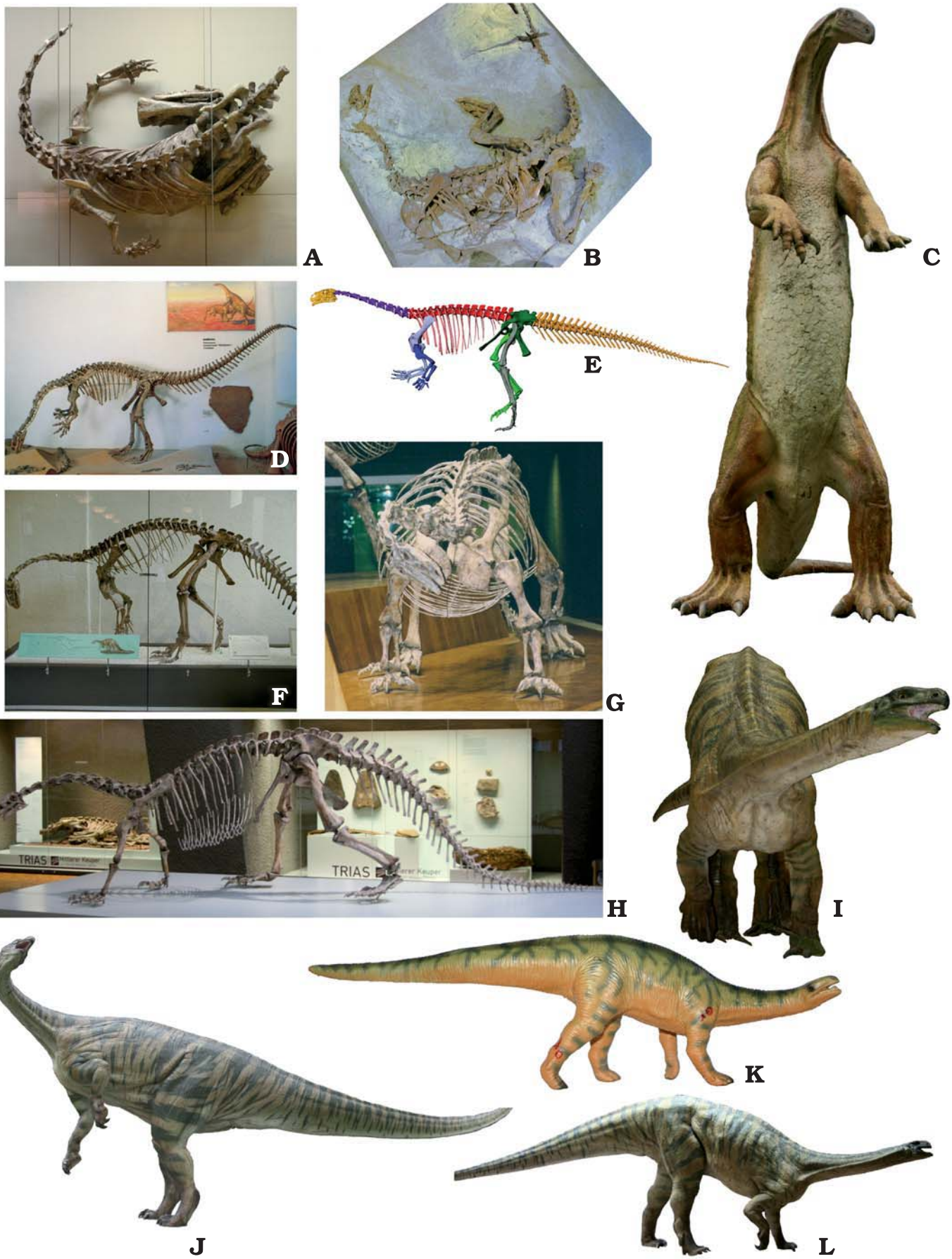

clusion of such a drawing in publications has almost become *de rigueur*. A certain standard has developed: the animals are depicted in lateral view, with the bones drawn as outlines, and a suggested body outline surrounding them in black. Other views, dorsal, anterior or cross-sections, are sometimes also provided (e.g., Paul 1996, 2000). Some artists and researchers offer "rigorous" drawings of specific specimens, in which the preserved parts are hatched (e.g., Wellnhofer 1994), so that the viewer can judge what is actually know from the fossil and what is inferred from other finds of the same or similar species. This distinction is not moot, as shown by Therrien and Henderson (2007), because many animals do not scale linearly compared to their close relatives, so that linear scaling will deliver inaccurate size and mass estimate.

The first reconstruction drawing of *Plateosaurus* can be found in Jaekel (1913–1914). Most famous, though, is the drawing in Huene (1926: pl. 7). It depicts SMNS 13200, a nearly complete skeleton of *"P. quenstedti"*, a junior synonym to *P. engelhardti* (Galton 1985). The animal is shown in lateral view, in a bipedal pose with a steeply inclined body, apparently running quickly. Galton wrote a series of publications on *Plateosaurus* and related prosauropods, several of which (Galton 1971b, 1986a, 1990, 2000, 2001) also contain lateral view drawings. Those in Galton (2000) and (2001) are copies of that in Galton (1990), which is based on Huene (1926), as stated in Galton (2001) and some print editions of Galton (2000). The drawings in Galton (1971b) and (1976) are exact depictions of the museum mount of AMNH 6810. Weishampel and Westphal (1986) published a guide to the *Plateosaurus* exhibit in the IFGT, which contains a drawing in lateral view. Wellnhofer (1994) describes material from Ellingen in Bavaria. His "rigorous" drawing depicts *Plateosaurus* in a quadrupedal pose, with a tail base bent sharply downward. *Plateosaurus* receives an extensive figure treatment by Paul (1987, 1997, 2000). A lateral view of the skeleton with body outline, apparently in a rapid walk, is supplemented by a dorsal view and a drawing combining an anterior view at the level of the pectoral girdle and a posterior view at the level of the pelvic girdle, in the same pose. A second lateral view portrays the animal as a musculature reconstruction in a full gallop, with the pedes almost overstepping the manus. On request, Scott Hartmann (www.skeletaldrawing.com) provided a restoration drawing in lateral view. Skeletal restorations discussed below are reproduced in Fig. 2.

The public's perception of an extinct animal is shaped more by mounted skeletons in museums than by scientific publications. Due to the distribution of *Plateosaurus* throughout Central Europe, mounted skeletons or casts can be found in Frick (MSF), München (BSPG), Tübingen (IFGT), Stuttgart (SMNS), Frankfurt (SNG), Halberstadt (MHH) and Berlin (MFN). The IFGT houses two mounts. GPIT1 (Fig. 1D), the source data for the virtual skeletal mount (Fig. 1E) employed in this study, is a nearly complete individual mounted in a bipedal standing pose, snout close of the ground as if feeding or drinking (see Gunga et al. 2007; Mallison 2007, 2010). GPIT2 is a composite of similar size to GPIT1. It consists of two individuals, one consisting of a skeleton nearly complete to the level of the last dorsal, the other lacking all parts anterior to the pelvis. Several copies of mounts can be found in other museums worldwide. Some of the mounts have been altered or taken down in recent years. For example, the SMNS housed a total of four mounted casts of SMNS 13200, in a variety of poses (Ziegler 1988: cover illustration, fig. 4; Moser 2003: fig. 4). All but one in a quadrupedal walking pose (Fig. 1H, G) have been taken down for an exhibition redesign in 2007. Similarly, the MFN mount has been dismantled and not been recreated because of a museum renovation in 2006/2007. The lizard-like sprawling old mount of SMNS 13200 (Fraas and Berckhemer 1926) in the old Stuttgart museum was dismantled during World War II and never remounted. Outside Europe, the AMNH mount of a nearly complete Trossingen skeleton (AMNH 6810; Fig. 1F) from the joint 1921–1923 excavation has been used by most US researchers as the typical *Plateosaurus*. I here only discuss mounts that I was able to inspect personally, including mounts that have since been taken down, as reliance on photographs alone is prone to cause errors.

Even more memorable than drawings or mounts, but more difficult to assess for their accuracy, are models of the living animal. In a tradition going back to Benjamin Waterhouse's plaster dinosaurs created for Richard Owen in 1851 and exhibited in the Crystal Palace (London, UK), many museums today enliven their exhibits with life-sized models. In the SMNS, the old skeletal mounts were accompanied by two models, one in a tripodal (Fig. 1C) and one in a quadrupedal pose, at the scale of the largest *Plateosaurus* ever found. Together with the new skeletal mounts, new 3D models were set up in 2007, in quadrupedal (Fig. 1I, L), bipedal (Fig. 1J) and a resting pose. Additionally, toy versions of the old tripodal and the new quadrupedal (Fig. 1K) models (by Bullyland™) are available, which were created in collaboration with scientific advisors from the SMNS. While their small size leads to inaccuracies in some areas for technical reasons, they are overall proportioned almost like the life-sized models. They can stand in their stead for the analysis here, because they can be digitized accurately and thus help avoid the inherent inaccuracies of photograph analysis due to perspective distortion.

In addition to these classic reconstructing methods, digital techniques have also been used in recent years. Gunga et al. (2007, 2008) used high resolution laser scanning to obtain

← Fig. 1. Prosauropod *Plateosaurus engelhardti* Meyer, 1837 skeleton mounts and life reconstructions. **A**. SMNS F33, in position as found. **B**. MSF 23, in position as found. **C**. SMNS old tripodal model. **D**. GPIT1. **E**. GPIT1 virtual mount based on CT data. **F**. AMNH 6810. **G**, **H**. SMNS 13200 (cast). **I**, **L**. SMNS new quadrupedal model in anterior (**I**) and lateral (**L**) views. **J**. SMNS new bipedal model. **K**. Toy model of SMNS new quadrupedal model by Bullyland™. All but I femur/thigh length ~0.6 m, I ~5 m high. Photographs by the author except C ©GPIT. A, C–K from Trossingen, Germany, B from Frick, Switzerland.

doi:10.4202/app.2009.0075

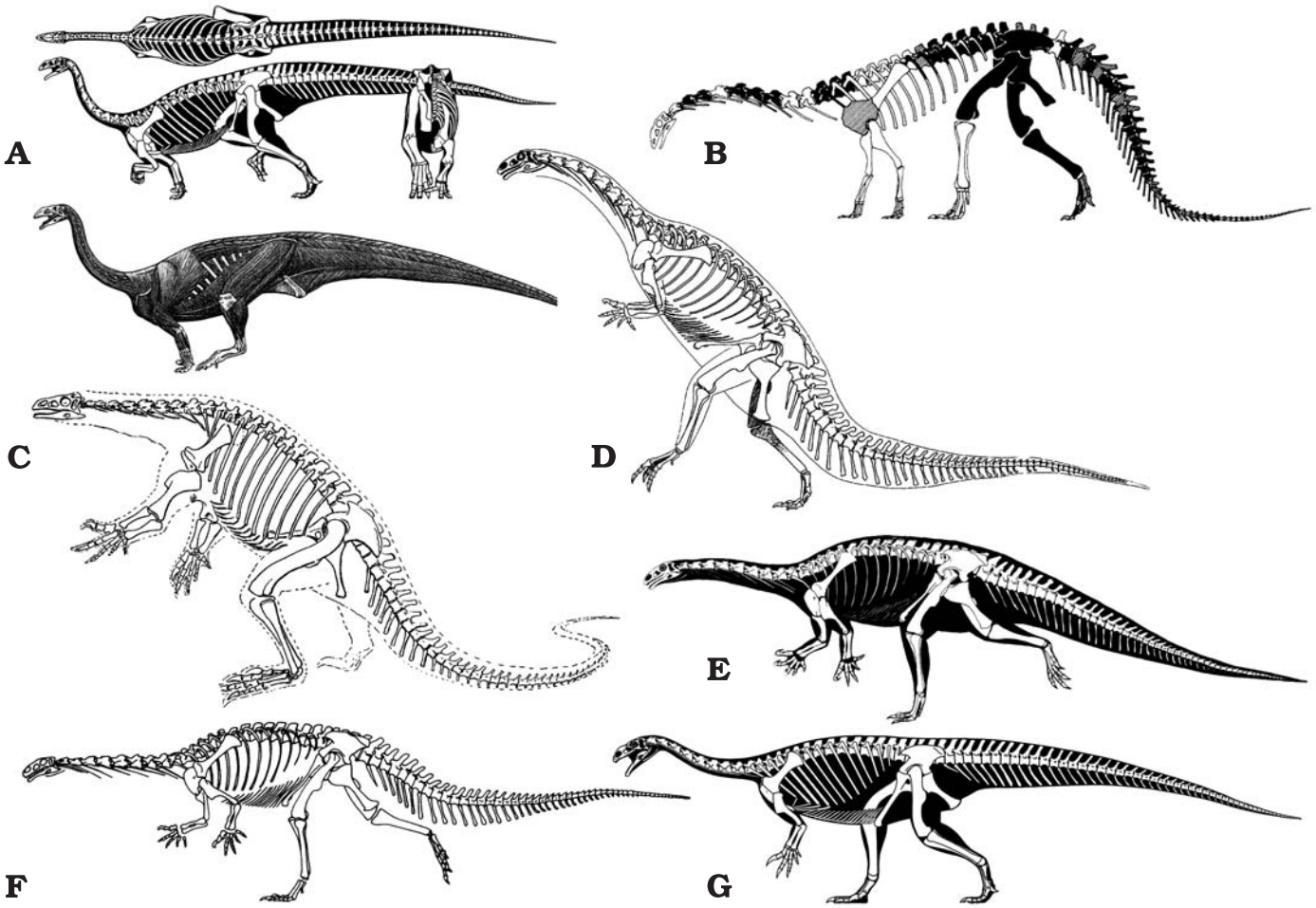

Fig. 2. Skeletal reconstructions of prosauropod *Plateosaurus engelhardti* Meyer, 1837, redrawn from: **A**. Paul (1987, 2000). **B**. Wellnhofer (1994). **C**. Jaekel (1913–1914). **D**. Huene (1926). **E**. Galton (1990). **F**. Weishampel and Westphal (1986). **G**. Scott Hartmann. (www.skeletaldrawing.com). Typical femur length of *Plateosaurus* is 0.6 to 0.8 m.

3D point cloud models of various mounted skeletons, including the mount of GPIT1 in the IFGT. Based on this excellent base they created two versions of a digital 3D model, one intentionally fat, the other slim, to assess the possible range of soft tissue reconstruction.

With all kinds of reconstructions it is important to provide a high level of accuracy. Pictures and models tell an "at one glance" message about an animal's body shape and proportions that immediately tells the viewer much more than just the shape and sizes of the actual (bony) specimen. Small inaccuracies can lead to drastic misinterpretations. A simple example is Henderson (2006), who used a drawing by Paul (1987) to create a 3D model of *Plateosaurus*, based on which the total mass and the center of mass position were calculated. For unknown reasons, the scale bar in the figure by Paul (1987: 29) appears in altered form in Henderson (2006: fig. 11). In fact, the size of the animal is considerably reduced by this small change, so that Henderson calculates a body weight of only 279 kg for *Plateosaurus* (Henderson 2006: table 4). The scaling difference is not immediately visible, so that there is a high risk that other researchers will use Henderson's mass value as the body weight of an adult *Plateosaurus* in future works. Similarly, the many drawings and skeletal mounts of *Plateosaurus* in a quadrupedal posture have led to an increasing number of artists' reconstructions in similar poses. Today the internet is a prime research tool for scientists and laypeople alike. Practically every internet site offers pictures with their text (or vice versa), and there is the increasing trend to reduce the text and emphasize the visual presentation. This means that pictures gain in importance relative to textual descriptions. Thus, inaccurate figures can have a profound influence on both the public's and the scientific community's perception of an extinct animal, and should be avoided at all cost.

An animal's range of motion, especially in limb joints, determines motion capabilities such as grasping ability or possible stride length. For an assessment of locomotion capabilities, it is of paramount importance to consider the motion ranges of the humerus and femur, as well as the ability to pronate the hand. Also, the lateral stiffness or flexibility of the vertebral column can provide insight into the animal's ability to use undulating motions for locomotion, either on

land or in water, while dorsoventral bending influences stride length during galloping and leaping. To date, detailed discussions of the mobility of extinct dinosaurs are limited almost exclusively to theropods, with an emphasis on their forelimbs (e.g., Galton 1971a; Carpenter and Smith 2001; Gishlick 2001; Carpenter 2002; Senter and Robins 2005; Senter 2006a, 2006b; Senter and Parrish 2006). Sauropodomorphs are rarely treated in detail, with the exceptions of, for example, Galton 1971a (*Plateosaurus*), or the discussion of manus pronation capabilities in *Plateosaurus* and *Massospondylus* in Bonnan and Senter (2007).

Here, I address the mentioned reconstruction drawings, mounts and 3D models with regards to accuracy, attempting to determine which factors have the strongest influence on accuracy. Also, I test claims about joint motion range, using the 3D virtual skeleton of GPIT1. This method is much easier to use than manual manipulation of casts or real bones, as e.g., conducted by Senter and Robins (2005). Aside from allowing extensive study without the risk of damaging the specimens, it also can be performed without access to the material, once it has been digitized. Also, there is no need to create elaborate support for the bones in larger assemblages (see Senter and Robins [2005: fig 1] for an example concerning a theropod forelimb). Claims about motion range can be explicit, e.g., Paul (2000: 83): "[in] most bipedal dinosaurs […] the lower arm bones, radius and ulna, could rotate around each other", they can be implicit in a drawing (e.g., showing a strongly dorsiflexed neck), or even in a remark on locomotion or behavior of the animal, e.g., Paul (2000: 91): "The long-backed prosauropods may have run with a bounding gallop, but the heavily built, shorter-footed melanorosaurs probably galloped less and trotted more". This implies that *Plateosaurus* was capable of quadrupedal locomotion, did not have a sprawling gait, and could use gaits with unsupported phases.

Institutional abbreviations.—AMNH, American Museum of Natural History, New York, USA; BSPG, Bayerische Staatssammlung für Geologie und Paläontologie, München, Germany; GPIT, see IFGT; IFGT, Institut für Geowissenschaften, Eberhardt-Karls-Universität Tübingen, Tübingen, Germany (collection numbers: GPIT); IPFUB, see FUB; FUB, Freie Universität Berlin, Germany (collection numbers of osteological collection IPFUB OS); MB.R., see MFN; MFN, Museum für Naturkunde – Leibniz-Institut für Evolutions- und Biodiversitätsforschung an der Humboldt-Universität zu Berlin, Berlin, Germany (collection numbers: MB.R.); MHH, Museum Heineanum Halberstadt, Halberstadt, Germany; MSF, Sauriermuseum Frick, Frick, Switzerland; SMA, Sauriermuseum Aathal, Aathal-Seegräben, Switzerland; SMNS, Staatliches Museum für Naturkunde Stuttgart, Stuttgart, Germany; SNG, Senckenbergische Naturforschende Gesellschaft, Frankfurt, Germany.

Other abbreviations.—ONP, osteologically neutral pose. Two vertebrae are in ONP if their centra faces are parallel and the zygapophyses overlap fully.

Material

For creation of the virtual mount of *Plateosaurus*, the nearly complete individual GPIT1 was CT-scanned at the UHT by Burkhard Ludescher. Scanning and file extraction details are given in Mallison (2010). Several elements of GPIT1 are missing or severely damaged. Where possible these were replaced with CT-scan based files from GPIT2, a composite skeleton from the same excavation and of similar size (see Huene 1926, 1928, 1932). These include the whole left manus, and in order to avoid misinterpretations on the proper articulation and the motion range of the wrist, the entire left forelimb of GPIT2 was used. Also, the left pes was mirrored and used in stead of the right pes, in which most metatarsals are incompletely preserved. Several elements are missing in both GPIT1 and GPIT2, or so incompletely preserved that they are not useful for the work presented here. These are: both clavicles, all cervical ribs not attached to the cervical vertebrae, and the sternals. The gastralia could not be scanned due to being embedded in large sediment slabs. Results concerning missing, deformed or potentially deformed elements of GPIT1 and GPIT2 were compared to other individuals of *Plateosaurus*, both from Trossingen and Halberstadt. These include SMNS F33 (Fig. 1A), MB.R. 4429, an articulated neck with skull from Halberstadt, MSF 23 (Fig. 1B), and SMA unnumbered, an articulated neck with partial skull and the first six dorsals from Frick. These and other specimens, as well as the diagram of GPIT1 as found in the field by Huene (1928: pl. 10) were also used for assessing the correct articulation of the skeleton, especially the manus and pes, and the possible motion range of the neck.

The 3D files (Polymesh [*.stl] format) are available on request from the author, providing previous permission for use by the IFGT.

Methods

Computer programs and digitizer

All CAD tasks (mounting the skeleton, motion range analysis) were conducted using McNeel Associates Inc. "Rhinoceros® NURBS modeling for Windows®" versions 3.0 and 4.0. Digitizing of toy models also took place in Rhinoceros©, using an Immersion™ Microscribe 3D digitizer. The resulting point clouds were meshed in Geomagic Inc. Geomagic Qualify 8.0© (time limited evaluation version).

Methods of CAD virtual skeleton creation and range of motion assessment

The virtual skeleton of GPIT1 was created in a bipedal standing pose (Mallison 2010). For the assessment of mobility, those elements of importance to the joint being investigated (e.g., two consecutive vertebrae or humerus, radius and ulna)

doi:10.4202/app.2009.0075

were copied into a new Rhinoceros® file. One object was given a different color and made immobile ("locked"), the other one duplicated and moved to an extreme position (e.g., maximum dorsiflexion). Other copies were moved into further extreme position (e.g., extreme lateral flexion) until all possible positions had been created. Combinations of extremes (e.g., maximum lateral flexion at maximal dorsiflexion) were also created. Throughout the process, the articulation of the elements was checked in six axial views and a freely rotatable perspective view. Where necessary, objects were made translucent to allow better judgment of the feasibility of the created articulation. Angles were measured in the CAD program either directly using bone landmarks, or by adding a line to the bone before motions were tested, copying and moving this line with the bone, and then measuring the angle between the two lines. The resulting files for each motion between vertebrae were imported into one new file, to illustrate e.g., maximum dorsiflexion of the entire dorsal vertebral column. Similarly, for the limbs the files from stylopodium, zeugopodium and autopodium were united. Here, all non-redundant positions were combined, to illustrate the total motion range of the limb.

Motion between vertebrae was assumed to be possible if any zygapophysal overlap was retained. This means that in contrast to Stevens and Parrish (1999, 2005a, b), 50% overlap is not required. Stevens and Parrish (1999) use this value, but as they point out (Stevens and Parrish 2005a), giraffes retain only minimal overlap, and avian cervicals retain between 25% and 50% of overlap. Here, minimal overlap is therefore used, and the resulting position then assessed for its feasibility. Overlap of 50% is used when higher values lead to unrealistic results as mentioned below.

Influence of soft tissues on the range of motion

Ligaments, muscles and tendons.—Aside from the bones, soft tissues have a large influence on the motion range of joints. For example, ligaments play an important role in blocking or strictly limiting certain degrees of freedom in many joints (McGinnis 2004; Stevens and Parrish 2005a). Sometimes these limitations are obvious from the bone shapes. For example, the shape of the distal condyles of the human femur indicates that the knee is, as a first approximation, limited to flexion/extension only, even though the bones alone would allow other motions such as antero-posterior sliding. Similarly shaped femora in extinct animals can thus be assumed to have had a similar complement of ligaments, and the knee therefore a similarly limited amount of degrees of freedom. If insertion sites of ligaments can be found on the fossil, and the corresponding ligament in extant taxa reliably identified, the accuracy of a motion range analysis can increase, but in the case of *Plateosaurus* few traces were found, and no corresponding ligaments could be identified with certainty.

Muscles and their tendons can also limit motions (McGinnis 2004), because they cannot be stretched at will. The greater the distance between a muscle's path and the joint it works on, the lesser the angle the moved body part can cover. The prime example is the caudofemoralis longus muscle, running from the underside of the anterior tail to the fourth trochanter of the femur. Its moment arm on the hip is accordingly large, and the more distal position of the fourth trochanter in dinosaurs compared to lizards and crocodiles means that the angle the femur can cover is smaller. The exact rotation angle, however, depends on many unknown variables, among them the internal structure of the muscle (parallel-fibred or pennate?), the relative length of its tendon, and the path both take through other soft tissues, so that the resolution that can be achieved by modeling the muscle is insufficient to be of help for a range of motion study (contra Paul 2005). In such cases evidence from skeletons found in life-like positions can help determine minima for joint deflection angles. Many skeletons of *Plateosaurus* were found belly down, with strongly flexed hind limbs, e.g., MSF 23 (Fig. 1B) and especially SMNS F33 (Fig. 1A). Although sediment compaction has compressed SMNS F33 to the point where the femur, tibia and metatarsus are in contact with each other along the bone shafts, it is reasonable to assume that *Plateosaurus* could indeed adopt a resting pose in which the pelvic girdle supported part of the animal's weight. SMNS F33 can be used to reconstruct this position, by attempting to place the digital skeleton into the same pose without disarticulating any joints. Where this is not possible the digital bones must be placed in the closest possible position that is dorsoventrally of greater extent, because SMNS F33 was mainly dorsoventrally compressed. The resulting pose of the digital skeleton (see below) is then the best estimate for the posture SMNS F33 had before sediment compaction. The resulting protraction angle of the hind limb and the flexion angle of the knee and ankle are required minima. In the following, if angles determined using this or similar approaches are smaller than those suggested by bone-bone articulation, the smaller angle is given.

Motion range limitations are especially important and difficult to determine from the bones alone where muscles or tendons cross more than on joint. The maximum length of the muscle may be insufficient to allow full range of motion in all joints, effectively reducing the range of motion, while single-joint muscles rarely do so (McGinnis 2004). For example, *Crocodilus porosus* (IPFUB OS 13) shows limits of about 13° per joint in the tail for lateral flexion based on the bones alone at 50% zygapophsal overlap and 22° with minimal overlap, but is limited to roughly 6° per joint when the complete tail is flexed to one side, based on measurements of overall curvature of the tail on photographs (Fig. 3A; own unpublished data). In contrast, if the tail is placed in a sinusoidal curve, so that e.g., only ten articulations flex to the left, and the following ten flex to the right, the soft tissues do not reduce the maximum angle as much, allowing 10° of motion per joint (own unpublished data). The osteoderms of crocodiles have an even larger influence blocking flexion and extension of the trunk. Overall, *Crocodylus porosus* is capable of roughly a 45° extension in the dorsal series (own unpublished data), while the vertebrae alone would allow more

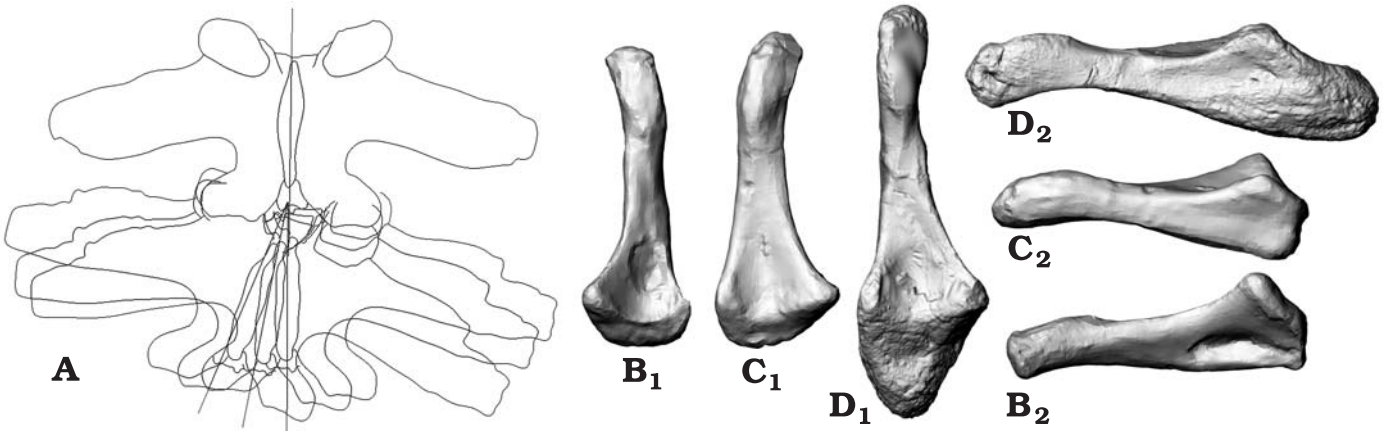

Fig. 3. Examples for the influence of soft tissues on joint motions. **A**. Outline drawing of caudals 5 and 6 of salt-water crocodile *Crocodylus porosus*, IPFUB OS 13 in dorsal view. Anterior is up. Caudal 6 is shown in positions with full, 50% and minimal zyapophysal overlap (0°, 10°, 21°, respectively). Width of caudal 5 across transverse processes is 113 mm. **B**–**D**. Ulnae of stegosaur *Kentrosaurus aethiopicus* Hennig, 1915 from the Upper Jurassic Tendaguru Formation of Tanzania, in anterior (B_1–D_1) and lateral (B_2–D_2) views. Right (**B**, field number St [unknown]) and left (**C**, field number St 113) ulnae, both part of GPIT 1424 (mounted skeleton). **D**. Left ulna (part of skeletal mount in MFN) MB.R.4800.33 (length 306 mm) shows cartilage preservation on the distal and especially proximal end, preserving a large olceranon process.

than 90°. The influence of soft tissues on the motion range of a joint depends on many factors, and cannot be taken into account in detail here, especially because there is no direct fossil evidence of soft tissues known in *Plateosaurus*.

Articular cartilage.—Especially difficult to estimate is the influence of articular cartilage on joint motion. In many joints of dinosaurs, including *Plateosaurus*, the amount of cartilage was small, comparable to extant mammals and birds. Especially in the digits and along the vertebral column there are well developed bony articulation surfaces, so that good matches exist between the bones. However, the ends of limb bones as well as the articular edges of e.g., the scapulae, coracoids and sternals retained a large amount of cartilage, so that the shape of the preserved bone may not correlate closely to the actual articulation surface. In general, there appears to be a good correlation of the general shape and main features (but not the fine details) in adult archosaurs, but juveniles of all and adults of some selected taxa show massive differences (Bonnan et al. 2009; own unpublished data). Cartilaginous tissues are rarely preserved on fossils, so the thickness of cartilage caps in dinosaurs is unclear. Often, it is claimed that even large dinosaurs had only thin layers of articular cartilage, as seen in extant large mammals, because layers proportional to extant birds would have been too thick to be effectively supplied with nutrients from the synovial fluid. This argument is fallacious, because it assumes that a thick cartilage cap on a dinosaur long bone would have the same internal composition as the thin cap on a mammalian long bone. Mammals have a thin layer of hyaline cartilage only, but in birds the structure is more complex, with the hyaline cartilage underlain by thicker fibrous cartilage pervaded by numerous blood vessels (Graf et al. 1993: 114, fig. 2), so that nutrient transport is effected through blood vessels, not diffusion. This tissue can be scaled up to a thickness of several centimeters without problems.

An impressive example for the size of cartilaginous structures in dinosaurs is the olecranon process in the stegosaur *Kentrosaurus aethiopicus* Hennig, 1915. In the original description a left ulna (MB.R.4800.33, field number St 461) is figured (Hennig 1915: fig. 5) that shows a large proximal process. However, other ulnae of the same species lack this process, and are thus far less distinct from other dinosaurian ulnae (Fig. 3B, C). The process on MB.R.4800.33 and other parts of its surface have a surface texture that can also be found on other bones of the same individual, and may indicate some form of hyperostosis or another condition that leads to ossification of cartilaginous tissues. Fig. 3B–D compares MB.R.4800.33 and two other ulnae of *K. aethiopicus* from the IFGT skeletal mount. It is immediately obvious that the normally not fossilized cartilaginous process has a significant influence on the ability to hyperextend the elbow, because it forms a stop to extension. Similarly large cartilaginous structures may have been present on a plethora of bones in any number of dinosaur taxa, so that range of motion analyses like the one presented here are at best cautious approximations.

Methods for comparing the virtual skeleton to previous reconstructions

For comparison of a reconstruction drawing to the virtual skeleton, the drawing was imported into Rhinoceros© as a background image and scaled to fit the virtual skeleton. If possible, a fit was created for the overall length of the dorsal series and the femur length. If this was not possible due to differences in proportion, the dorsal series alone was used. Initial attempts to include the sacral series as well failed, because of different deformations of the sacra of GPIT1 and SMNS 13200, the latter of which is the base for most reconstruction drawings. If there were several views of a recon-

doi:10.4202/app.2009.0075

struction available, they were imported into one Rhinoceros© file and arranged as background images in the appropriate axial viewports (dorsal view in the "top" viewport, anterior view in the "left" viewport, etc.). The virtual skeleton was then posed to conform to the drawing as well as possible. In case of length differences between bones, the virtual bone was shifted to the proximal/anterior end of the corresponding element in the drawing, creating a visible gap in the next distal articulation. Ribs were ignored in most cases, due to the relatively high degree of deformation in the ribs of GPIT1, and the usually quite schematic style of the ribs in the drawings. The sole exception is the set of drawings by Paul (1987, 1997, 2000). Paul considers his drawings "technical reconstructions", even when they are based on old photographs of mounts, and uses them for taxonomic investigations (Paul 2008). Clearly, these drawings must thus conform to higher standards than others that are created purely for illustrating general proportions of the animal. In the case of multiple views, the bones were first arranged according to the lateral view, then in the other views. If this required misaligning them in lateral view, a duplicate was created instead. The resulting pose was assessed in all axial and the perspective views.

Skeletal mounts in museums were inspected for correct articulation visually and on photographs. Because several mounts were visited several years ago, before the conception of the work presented here, and have since been dismantled, their assessment was based on photographs alone. Here, and for life-sized 3D models, the problem of edge distortion had to be solved. Where possible, a number of photographs were taken with a 50 mm lens from a fixed distance at a right angle to the long and transverse axes of the mount or model, a 25% frame cut away from them, and the remaining, least distorted central parts combined into a composite image. Alternatively, a 300 mm lens was used to take one picture at a large distance. While these photographs are more distorted than a composite picture, they are better than a wide angle shot from a short distance.

One problem that could not be solved easily unless at least two orthogonal views were available is that of perspective distortion in dynamically posed mounts. If, e.g., the neck or tail curves towards or away from the viewer, they will appear shorter than they really are. This effect is hard to judge in lateral view alone. Where no picture from another perspective was available, I forced the virtual skeleton to fit the lateral view. This may hide articulation errors in the mounts or scaling errors in the models.

The digital 3D models were imported into Rhinoceros© directly, while the toy models were first mechanically digitized using the point cloud digitizing procedure detailed in Mallison at al. (2009), and meshed to create a 3D body in Geomagic Qualify 8.0©. The virtual skeleton was arranged to conform to them in the same way as for multiple view drawings. The 3D models by Gunga et al. (2007) were compared directly to the point cloud scan file of the IFGT GPIT1 skeletal mount, on the basis of which the models were created.

Results

Range of motion

In the following, maximum motion ranges with (where necessary) considerations of forces acting on articulations will be discussed for separate functional body units, such as the hindlimb or the tail. Note that the determined motion ranges are the extremes possible for these parts alone, not for the entire skeleton. In some joints, motions are possible to degrees that are blocked by other body parts given certain articulation angles of other joints. These combined motion ranges are discussed afterwards.

Vertebral column: cervical series.—*Plateosaurus* has 10 cervical vertebrae (plus a rudimentary proatlas), 15 dorsals and three sacrals (Huene 1926). Huene (1926) also lists 41 preserved and at least 15 missing distal caudals for SMNS 13200. In GPIT1 45 caudals are present, and only a very small number may be missing at the tip of the tail. Atlas and axis of GPIT1 are attached to the skull and were not available for CT scanning. For reference, the cervical column was placed so that the neural canal of the last vertebra was horizontal. The neck was mounted in neutral pose (following Stevens and Parrish [1999], the pose with perfectly overlapping zygapophyses and parallel centra faces is often also termed osteologically neutral pose [ONP]), although there are strong indications that the posture has no special significance for an animal's habitual posture (Christian and Dzemski 2007; Taylor et al. 2009). In lateral view the neck then projects upwards slightly, forming a 7° angle between the horizontal and the line connecting the posterior opening of the neural canal on the last and the anterior one on first preserved cervical. However, there is no marked angling of the centrum-centrum articulations at the base of the neck, nor marked keystoning. Rather, the centra are trapezoidal in lateral aspect, with the anterior face dorsally displaced in relation to the posterior face. This shift is present in all but the first two cervicals, "stepping up" the neck while the intervertebral discs are parallel to each other. The anterior three cervical centra are slightly keystoned, creating a ventrally concave arch that places the anterior surface of the centrum of the epistropheus in a near vertical position. The shape of the atlas and its articulation with the epistropheus result in a downwards inclined position of the skull, as described by Huene (1926: 28).

Any definitive assessment of neck mobility requires knowledge of the shape and potential flexibility of the cervical ribs. These, however, are not fully preserved in GPIT1 today, and have not been prepared separately in other individuals of *Plateosaurus*. Several articulated necks have been retained in the position they were found in. Especially well preserved are SMNS F33, SMA unnumbered, and MB.R.4429. Of these, SMNS F33 and MB.R.4429 curve strongly, are well articulated, and their cervical ribs are distally slightly bent, indicating some flexibility in vivo. Although the cervi-

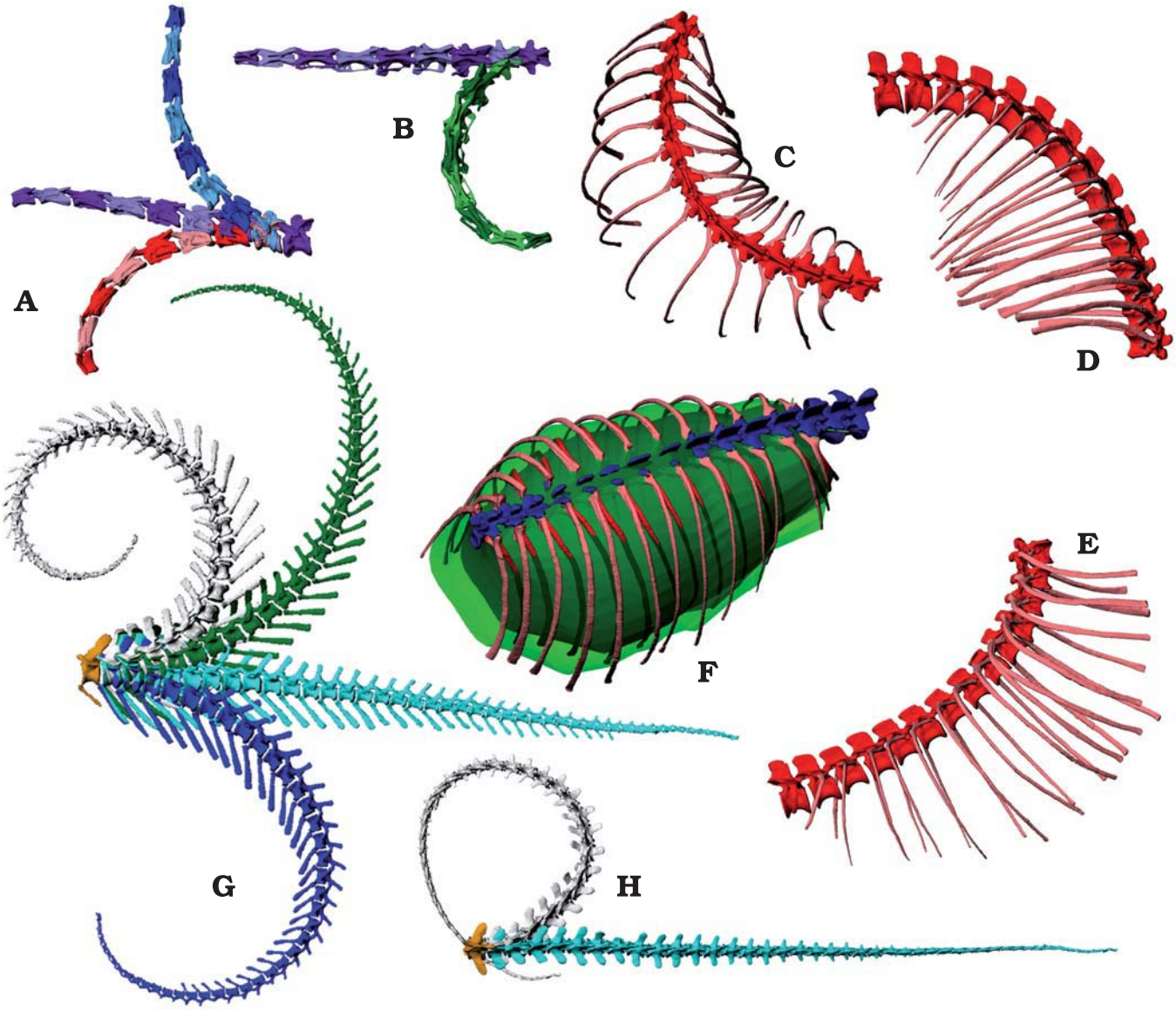

Fig. 4. Range of motion of prosauropod *Plateosaurus engelhardti* Meyer, 1837 using the digital skeleton mount of GPIT, from Trossingen, Germany. **A**. Lateral view of cervicals in neutral articulation, maximal dorsiflexion and maximal ventriflexion. **B**. Dorsal view of cervicals in neutral articulation and maximal lateral flexion. **C**–**F**. Dorsal vertebral column and ribcage in dorsal view in maximal lateral flexion (**C**), lateral view in maximal ventriflexion (**D**), lateral view in maximal dorsiflexion (**E**); air exchange volume determination (**F**). Pink ribs and dark green volume = exhaled volume, red ribs and translucent green volume = inhaled volume. See text for further explanation. **G**. Tail in lateral view, showing (top to bottom) dorsiflexion at 10° and at 5° per joint, neutral articulation, maximum ventriflexion. **H**. Tail in dorsal view, straight and at 10° lateral flexion. Length of cervical series 103 cm, length of dorsal series 137 cm, length of caudal series 261 cm. Anterior to the left in A–C and F–H, to the right in D and E.

cal ribs in *Plateosaurus* overlap the next vertebra, it is unlikely that they blocked intervertebral motion. For the digital analysis presented here I therefore ignored them, instead comparing my results to the articulated necks.

Ventral mobility of the neck is limited to a 100° curve, measured as the angle between the anterior face of cervical 2 and the posterior face of cervical 10. Mobility is greatest between the anterior vertebra, and decreases with the reducing length of the vertebrae posteriorly. In the posteriormost three cervicals, ventriflexion is minimal, both because of the dorsal displacement of the zygapophysal articulation, and the trapezoidal shape of the centra. Dorsiflexion is possible to a slightly larger extent (110°), with the posterior half of the neck contributing the largest part. The anterior part is in comparison quite stiff (Fig. 4A).

Lateral motions of the neck cannot be accurately judged because of the imperfect preservation of the cervical ribs. However, a 180° curve appears plausible as a minimum, placing the head 0.6 m laterally and 0.3 m above the neck base, with the snout pointing caudally (Fig. 4B). SMNS F33, MB.R.4429, and MSF 23 do not contradict this interpretation. All are less flexed than appears possible from the virtual mount, but all also appear not to be flexed to the limits of the intervertebral joints. An articulated neck in the SMA (unnum-

doi:10.4202/app.2009.0075

bered) from Frick shows a similar curvature as SMNS F33, although created by both dorsiflexion and lateral flexion. Galton (2001: fig. 1c) figures the skeleton of AMNH 6810 as found based on an unpublished drawing by Friedrich von Huene. Its neck is curved ~180°, with the largest flexion angles occurring in the middle part of the neck. However, it is not clear whether these vertebrae are still articulated. In all, it seems reasonable to assume that the values given above are possible, but a slightly more restricted range of motion cannot be ruled out. Torsion is almost totally blocked by the medially angled zygapophysal articulations along the entire neck.

Vertebral column: dorsal series.—ONP articulation creates a slight dorsally concave arch in the anterior five dorsals, and a slight ventrally concave curve in dorsals 6 to 10. From dorsal 11 on, the series is straight. As in SMNS 13200, the zygapophysal faces of GPIT1 are medially inclined about 45° between dorsals 1 and 2, measured by placing a rectangle on the articulation surface of each side in the CAD program, and having the program calculate the angle this plane forms with the vertical axis. From dorsal 3 on, the zygapophyses are oriented progressively less steep up to dorsal 6, where the angle is about 18°. Further posteriorly, they are oriented more steeply again, and reach approximately 35° between dorsal 15 and the first sacral. This angle is 10° lower than in SMNS 13200. It is unclear whether this difference is caused by intraspecific variation or deformation. The angles for GPIT1 were determined on the right side only, because the lateral processes and zygapophyses of the left side are all displaced dorsally by postmortem deformation. The zygapophysal alignment indicates a high mobility in dorsoventral direction in the posterior and even more so in the anterior third of the dorsal series. The middle part is somewhat less flexible in dorsoventral direction, and additionally allows strong lateral flexion. Torsion is blocked by steeply oriented zygapophyses, and thus only possible, to a limited degree, in the middle third of the dorsal series. Articulation of the digital files confirms this interpretation. However, lateral flexion of the vertebrae alone is possible to an extent that appears unreasonable, allowing nearly a full circle for the entire dorsal series. Lateral flexion between consecutive vertebrae of over 30°, as possible between, e.g., dorsals 7 and 8, leads to intersection of the ribs. Apparently, lateral motion in vivo is not blocked osteologically, but rather by the maximum compression of the intercostal tissues. Addition of the ribs to the 3D file leads to a maximum lateral curvature of the dorsal series of about 110° (Fig. 4C). Flexion is also blocked by the ribs, not the intervertebral articulations, allowing a 85° curve (Fig. 4D). Extension was limited by the intercostal and ventral soft tissues, the effect of which is difficult to determine. However, a 90° curve for the entire dorsal series seems possible (Fig. 4E). In life, the dorsal mobility of the anterior dorsals was certainly greater, as rib motion was ignored here. This would have increased the motion range of the neck by moving the neck base.

Ribcage.—The ribs of GPIT1 all show the marks of postmortem deformation and distortion. Comparison between contralateral elements shows that this damage is not significant enough to make a reconstruction of the ribcage width impossible. The capitulum can be matched accurately with the parapophysis in most ribs, but the dorsal displacement of the left transverse processes of many dorsal vertebrae results in a dorsal displacement of the diapophysis (term used here sensu Huene [1926] and Wilson [1999], referring to the articulation surface, not the entire transverse process). In some dorsals, the tuberculum cannot be articulated with it at all, in others the resulting position elevates part of the rib shaft as high as the top of the neural arch. Similarly, on the right side some neural arches, and with them the diapophyses, have been displaced ventrally. Here, the respective ribs are tilted medially. In the virtual skeleton an attempt was made to correct for these errors, placing the ribs as symmetrically as possible. This results in a high-oval ribcage cross-section, in which the transverse axis at the widest point (dorsal 6) is slightly shorter than the vertical axis, if the latter is measured from the ventral end of the corresponding rib. The 4th to 9th ribs are almost equal in length, and the cross sections only slightly less wide than in the 6th. Fitting an ellipse into the rib pairs of this region results in a ratio between the transverse and the vertical axis of 0.85. In the first to third rib pairs a greater difference exists between the axes of the ellipse, with the transverse axis roughly 0.6 times the length of the vertical axis. The posterior third of the ribcage is only slightly wider than the anterior third, but the ribs are much shorter. Their distal ends form a posteriorly ascending line that corresponds to the pubes.

While the correct angle between the longitudinal axis of the animal and the rib shafts cannot be determined with ease, it is nevertheless possible to estimate the tidal volume of *Plateosaurus* on the basis of the reconstructed ribcage. As in tyrannosaurids (Hirasawa 2009), the ribs rotate around an axis defined by the articulations between capitulum and parapophysis, and tuberculum and diapophysis. The orientation of these axes is one of the main factors defining thorax kinematics. The axes of rotation were determined by creating cylindrical bodies that were arranged with one end touching the diapophysis and the other end the parapophysis. Five point objects were created on the medial side of each rib, splitting the medial face of the rib into four segments, and grouped with the rib, so that any motion of the rib also affects the points. All ribs were rotated around their respective articulation axes by +5°, while a copy of each rib (with the attached points) was rotated by -5°, creating a 10° difference between the two rib sets. This angle results in rib kinematics similar to those observed during rest or moderate activity in extant basal birds (Claessens 2009) or reconstructed for tyrannosaurids (Hirasawa 2009), with lateral displacement of the ventral end of the rib always surpassing ventral displacement. Based on the points on each rib, curves were created that in general terms follow the rib shape, forming U-shapes open ventrally. These were closed by creating a straight curve section closing the gap. From each set of curves, a NURBS body with straight sections was lofted, and

its volume determined (Fig. 4F). Similar bodies were also created for the neutral rib positions, and for rib rotations of +10° and -10°. The difference between the volumes for +5° and -5° rotation is almost 1900 cm^3, or 19 liters. Values for neutral to +/-10° are ~1500 cm^3 and ~2500 cm^3, so 2000 cm^3 appears to be a good average estimate of the tidal volume. While there is no reason to assume that all ribs rotated through the exact same angle during breathing, the approach chosen here is sufficient for a rough estimate of the air exchange volume, because small changes of the angle in the anterior and posterior ribs have only a minuscule influence on the volume. Altering the angle of the ribs in their supposed neutral position has only a minimal effect on the air exchange volume, and a strong posterior angling results in a biomechanically disadvantageous position of the anterior ribs, in which compressive stresses on the pectoral girdle would work to laterally compress the anterior body even further. Also, the flattened shafts in the anterior ribs only form a continuous curve if the ribs are angled close to the position chosen here. Tilting them posteriorly would lead to the attaching musculature creating torsion forces in the rib shafts.

Vertebral column: caudal series.—In GPIT1 the zygapophyses of the caudals are angled between 50° and 60°, blocking torsion of the tail as well as limiting lateral flexion to ~10° to 12° per intervertebral joint. Due to the large number and short length of the vertebrae, the tail can still cover a large arc (Fig. 4G, H), allowing a lateral divergence of the proximal ten caudals of about 45° form the long axis of the animal even if only a 5° lateroflexion per intervertebral joint is assumed. Flexion is blocked by the haemapophyses at an angle of roughly 7° per joint, rather than by the zygapophses. Except for the first two, the haemapophyses are at least as long as the corresponding vertebra is high, but are strongly posteriorly inclined. In all, the distance between the distal ends of the haemapophyses and the ventral rim of the centra makes up 45% of the height of the tail, emphasizing the relatively greater role played by the caudofemoral musculature in prosauropods compared to crocodiles, where the same distance corresponds to less than 30% of tail height (*Crocodylus porosus* IPFUB OS 13).The first twenty haemapophyses are distally slightly thickened, and from caudal 15 on they tend to show a slight posterior curvature, but there is no distinct change of shape at any point. Extension to values greater than 10° per intervertebral joint creates large gaps between the centra, but there is no osteological block below 17°, when the neural spines collide. However, at such an angle no room is left for soft tissues. Taking soft tissues into account, a maximum angle of 5° to 7° per articulation appears reasonable (Fig. 4G). Lateral motion was probably limited by soft tissues. The bones alone easily allow for lateral flexion between 7° and 10° per intervertebral joint with 50% zygapophysal overlap (Fig. 4H), which would allow the entire tail to curve over 360°. A sensible assumption is that mobility in vivo was comparable to extant crocodilians, in which the zygapophyses (except for those of the first 5 caudals, which are less steeply oriented) are angled medially at slightly smaller values (40° to 55°; *Crocodylus porosus* IPFUB OS 13), allowing the tail tip to barely touch the side of the body. This corresponds to joint lateroflexion values of about 6°.

Pectoral girdle.—Both clavicles of GPIT1 were preserved complete and nearly in articulation (Huene 1926: 41). The fact that they as well as the anterior margins of the coracoids were in contact when excavated in both GPIT1 and GPIT2 indicates that this position reflects in vivo articulation, as pointed out by Huene (1926). Other finds show a similar arrangement, with closely spaced coracoids, e.g., MSF 23 and SMNS F 33, as well as several individuals from Halberstadt (Germany, Jaekel 1913–1914). Medially touching clavicles were reported for the closely related prosauropd *Massospondylus* by Yates and Vasconcelos (2005). Therefore, the pectoral girdle formed a narrow U-shape, allowing little or no rotation of the scapula against the ribcage.

In GPIT1, the left coracoid is badly deformed. The anterior and dorsal margins of the coracoid have been folded medially, but the rest of the bone as well as its association with the scapula appears unremarkable. However, the right coracoid has a much weaker curvature in dorsal view, as does the right compared to the left scapula blade. Other coracoids of *Plateosaurus* show great variability in both the curvature and the angle they forms with the scapula (see Moser 2003). When constructing the virtual mount I used an average of the bones of GPIT1.

The exact position of the pectoral girdle on the ribcage is impossible to determine, because of several uncertainties. First of all, it is unclear how far cranially the midline of the pectoral girdle projected. Positions below the 8th cervical to the 2nd dorsal are theoretically possible. However, very caudal positions require rotating the ribs improbably far back, and very cranial positions create too much room for soft tissues between the scapulae and the ribs, or force an extremely dorsal position of the scapulae. This is problematic, because the dorsal ends of the scapula blades then project nearly as far dorsally as the tips of the neural spines. Only positions with the anterior edges of the coracoids below the last two cervicals appear possible (Figs. 1D; SOM 1 at http://app.pan.pl/SOM/app55-Mallison_SOM.pdf). Also, the angle between the scalupar blade and the vertebral column cannot be determined exactly, but an angle steeper than 45° for the long axis of the scapula seems likely (see Bonnan and Senter 2007; Remes 2008; Mallison 2010, in press). The resulting position with a far ventrally, anteriorly and steeply angled scapula is similar to that of sauropods (Remes 2008) and even highly derived ornithischians, as evidenced by an articulated *Triceratops* find (Fujiwara 2009).

Forelimb: shoulder.—The glenoid on both the left and the right scapulacoracoid in GPIT1 is a simple U-shaped trough, despite the massive deformation of the left element. This is also true of all other well preserved specimens that can unequivocally be assigned to the same genus as GPIT1 (GPIT2, SMNS13200, MB.R.4404, MSF 23, see Galton [2000]; Moser

doi:10.4202/app.2009.0075

[2003]). Therefore, humerus motion was limited to a simple rotation around an axis transverse to the scapula blade when significant forces acted on the glenoid. The narrow U-shape of the pectoral girdle and the curvature of the scapulacoracoid dictate that this transverse axis is angled between 35° and 50° medially compared to the long axis of the animal, depending on the exact arrangement of the pectoral girdle chosen. Similarly, the axis can be tilted medioventrally up to 15°, or run horizontal, depending on the dorsoventral position of the scapulae on the ribcage. In the articulation deemed most probable here (roughly the middle of possible scapular positions in anterior and lateral views), the axis is angled 45° medially in dorsal view, and horizontal in anterior view. Therefore, humerus protraction and retraction under load is limited to an anteromedial-posterolateral plane, displacing the elbow laterally during retraction (Fig. 5A, E). The humerus can only cover an angle of approximately 80° in extension and flexion (Fig. 5B, D). This angle is not split evenly by the orthogonal to the scapula long axis through the glenoid, but only 35° extend in front of it in GPIT1 (angle varies for other skeletons due to different deformation of the scapulacoracoids). Thus, the humerus cannot be protracted to a vertical position if the scapula is placed with the long axis steeper than 35°. However, angles lower than 45° for the scapula are unreasonable (Mallison 2010; see also Bonnan and Senter 2007; Remes 2008), so that humerus protraction to vertical was impossible.

Maximal abduction (humeral elevation) and adduction angles are difficult to determine, due to the large amount of cartilage that must have been present in the shoulder. The glenoid is 8.0 cm wide on both sides, while the humeral head measures 5.4 cm on the left and 5.5 cm on the right humerus of GPIT1. Therefore, cartilage made up around 15% of the anteroposterior extent of the humeral head, assuming that cartilage thickness was equal on the humerus and glenoid. More probably, this figure is too low, and the cartilage cover of the glenoid was much thinner than that of the humeral head. It is in any case moot to try to reconstruct the shape of the cartilage cap in detail. Following Senter and Robins (2005), Galton (1971a) and Gishlick (2001) I here assume that the extents of the preserved articular surfaces on each bone represent the limits of possible motion. Large abduction and adduction angles require the glenoid to be free of significant shearing forces, so that the forelimb can not have played a significant role in locomotion, which would require a sprawling position. Fig. 5A, C, E and SOM 1 (http://app.pan.pl/SOM/app55-Mallison_SOM.pdf) depict the maximum abduction and adduction angles that may have been possible under compacting forces. Larger angles were probably not possible if significant forces acted on the joint. Humeral elevation to the level of the glenoid is impossible expect at large retraction angles (i.e., not possible by abduction, Fig. 5A–D), but the manus can cross the body midline ventrally (Fig. 5A, E). Rotation of the humerus head in the glenoid, as seen in animals with a sprawling posture (e.g., *Alligator* and *Varanus* [Goslow and Jenkins 1983; Landsmeer 1983, 1984]), was probably very limited. In apparent contrast to the limited motion range, the wide proximal end of the humerus indicates that the shoulder musculature was voluminous and required large moment arms in *Plateosaurus*, similar to all other prosauropods (see Remes 2008), indicating a powerful forelimb.

Forelimb: elbow.—The axis through the distal condyli of the humerus is rotated against the transverse axis of the proximal end, which corresponds to the rotation axis in the glenoid, by about 30°, with the ulnar condyle displaced ventrally. This means that flexion and extension of the elbow occurs in a plane that is only slightly rotated against the median plane of the animal. Extension in the elbow is limited to slightly less than a straight position (which is here equivalent to 180°), the zeugopodium forming a nearly straight line with the stylopodium (Fig. 5B). Flexion is possible to at least 70° (Fig. 5B). For SOM 1 (http://app.pan.pl/SOM/app55-Mallison_SOM.pdf), I chose a spaced articulation between radius and ulna, in order to maximize pronation potential. Because of this, flexion to angles below 120° requires a supinating motion by 15° to sustain articulation between the radius head and the radial condyle.

Manus pronation by longitudinal rotation of the radius around the ulna is not possible to a degree that allows a ventral direction of the palm in *Plateosaurus*. The proximal articular end of the radius is much wider than the shaft, and strongly elliptical in proximal aspect (Fig. 5F, G) in contrast to, e.g., *Homo sapiens* and *Felis silvestris*. These species have a circular proximal radius head with a shallow circular articular pit, allowing rotation of the radius at all flexion angles of the elbow. In contrast, GPIT1 and all other individuals of *Plateosaurus* examined for this publication consistently exhibit a shallow trough, the curvature of which is the same or very similar to that of the proximal articular facet of the ulna (Fig. 5F). As with the glenoid, much cartilage must be missing from the elbow joint, so the possibility cannot be ruled out that cartilaginous structures allowed a modest amount of radius rotation. However, even assuming a rotation by 90° does not lead to manus pronation sufficient to allow the palm to face fully ventrally. Examination of extant taxa such as *Gorilla gorilla*, *Homo sapiens*, several species of *Manis* and *Felis cattus* (MFN collection) shows that the degree of rotation of the radius that is possible against the ulna can be reliably estimated by taking a photograph of the radius in proximal view and fitting a circle to the medial outline. The angle corresponding to the arc conforming to the medial outline of the radius head is somewhat greater than the maximum angle the radius can be rotated. In *Plateosaurus*, the corresponding angle is roughly 80° (Fig. 5G), 40° supinating and 40° pronating from the best fit between radius and ulna. This apparent neutral position is with the palms facing 60° medially from dorsal, thus a 40° rotation leads to medially directed palms at best. For SOM 1 (http://app.pan.pl/SOM/app55-Mallison_SOM.pdf), pronation capability was maximized by spacing radius and ulna as far apart as possible. Also, the radius rotates 55°, much more than possible. Despite this, the palm faces at best 10° ventrally of medially. These results confirm, together with

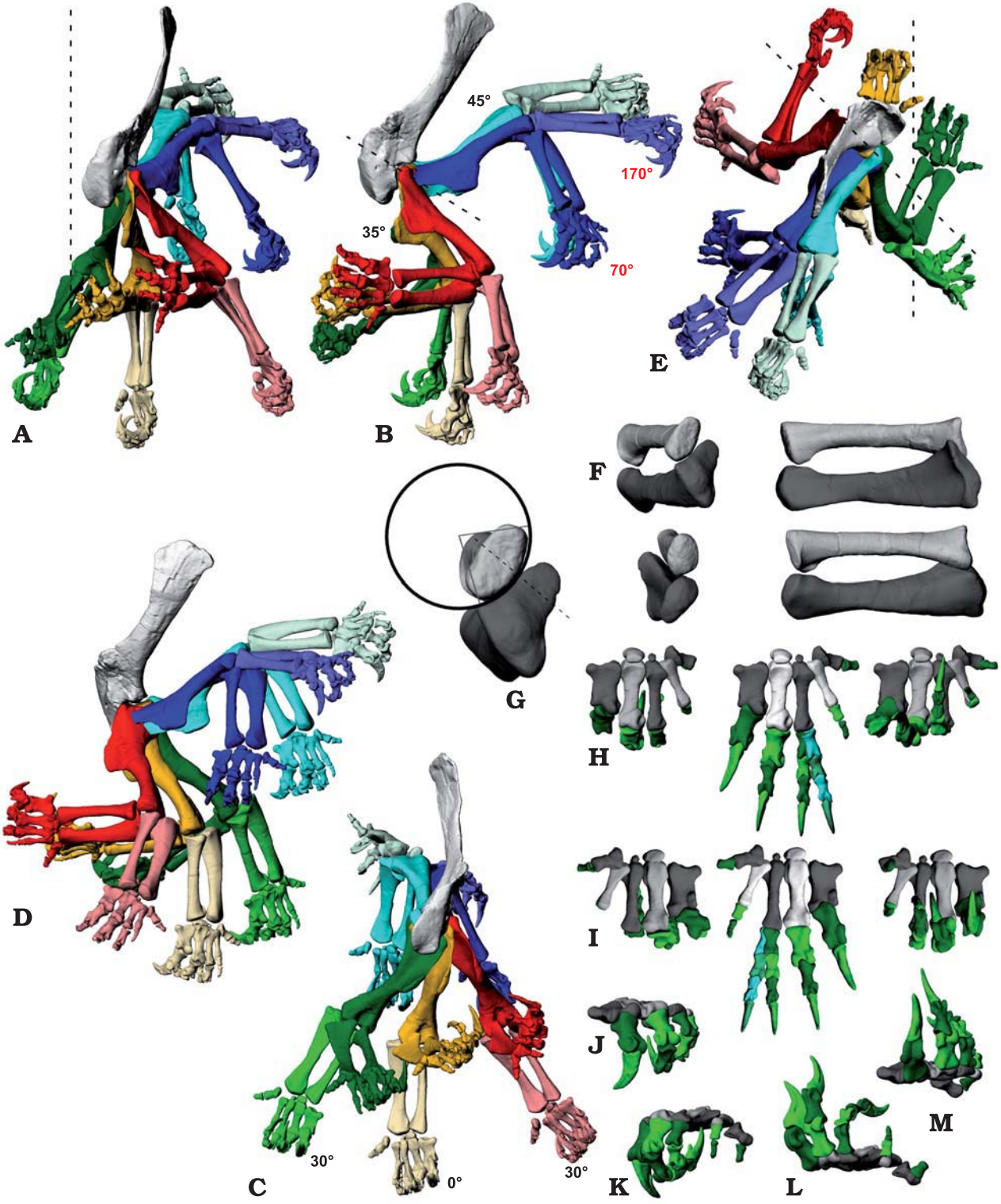

Fig. 5. Range of motion of the fore limb of prosauropod *Plateosaurus engelhardti* Meyer, 1837 using the digital skeleton mount of GPIT1, from Trossingen, Germany. **A**–**E**. Left scapula and fore limb in anterior (**A**), anterolateral (**B**), anteromedial (**C**), lateral (**D**), and dorsal (**E**) views. Equal colors are identical positions. B is parallel, C is perpendicular to the main axis (flexion/extension) of the glenoid. Length of humerus 350 mm. Dashed line(s) refer to: body midline (**A**), orthogonal to scapula blade long axis (**B**), body midline and main axis of glenoid (**C**). Red numbers in B refer to elbow, black to humerus flexion/extension. Numbers in C refer to humerus abduction/adduction versus the vertical. **F**. Left radius and ulna in articulation in (top row) proximo-lateral, medial view, (bottom row) distal and lateral views. Length of ulna 237 mm. **G**. Radius and ulna in proximal view. Dotted line indicates main joint axis of elbow. Circle and lines show method for determination of theoretical maximal pronation angle. **H**–**M**. Left manus. **H**, **I**. Left to right: flexion, neutral position and extension in dorsal (**H**) and palmar (**I**) views. Digit IV duplicated in neutral position views to show lateromedial deviation range. **J**–**M**. Oblique views of flexion (**J**, **K**) and extension (**L**, **M**). Length of metacarpal III 97 mm.

doi:10.4202/app.2009.0075

manual manipulation of specimens and digital manipulation of 3D data from several individuals (e.g., GPIT1, GPIT2, MB.R.4402, MB.R.4404), the results of Bonnan and Senter (2007), who studied AMNH 2409 exclusively. Bonnan and Senter (2007) also show conclusively that alternative methods for manus pronation, e.g., proximo-distal motions of the radius, are not possible in plateosaurid dinosaurs. Additionally, as pointed out by Mallison (2010), the posture of articulated skeletons in the field argues against *Plateosaurus* being capable of turning the palm ventrally without massive humerus abduction.

Forelimb: carpus, metacarpus and digits.—The block-like structure of the wrist appears to block rotating motions (see also Bonnan and Senter 2007), but to allow significant extension and flexion. The digits flex strongly, with the claws of digits II and III potentially able to touch the palm. In contrast to the description by Huene (1926), the digits are not widely splayed and the metacarpus does not show a significant transverse curvature. Only the whole of metacarpal V and the distal end of metacarpal 4 are placed clearly palmar in relation to the others (see also Jaekel 1913–14: fig. 20). This is a marked contrast to the tubular manus of sauropods (Bonnan 2003). The distal articular facet of metacarpal IV, however, is slightly tilted against those of metacarpals II and III. This directs the digits slightly medially during flexion. Digit III and especially digit IV also have some lateral mobility between the metacarpal and the basal phalanx, allowing lateral deviation and therefore some countering action of the flexed digit against digits I and II (Fig. 5G–J). The angle is quite limited at ~25°, comparable to the lateral mobility present in the digit IV of humans. Fully flexed, the digits can grasp around objects, and digit V opposes digits II and III (Fig. 5G–J, Mallison 2010: fig. 6). Digit I, as has also been pointed out for the closely related *Anchisaurus* by Galton (1976), is not angled strongly against digit II (Fig. 5G–K; Mallison 2010: fig. 6; contra Galton 1971a, b), and flexion reduces the angle to only 13° compared to the long axis of metacarpal III (Galton 1971a, b).

The right manus of SMNS F 33 is preserved in articulation, as is SMNS 13200 k, a right manus assigned to *Pachysaurus* by Huene (1932), a genus regarded as a junior synonym of *Plateosaurus* by Galton (1985). These two hands are the sole articulated prosauropod manus from the German Keuper preserved without significant transverse compression and whose elements have not been separated during preparation. In both, metacarpals II through IV are articulated with their shafts nearly parallel, forming an angle of less than 20°, and the entire metacarpus has no transverse arching. The visible parts of the bones do not suggest that this is a taphonomic artifact, confirming the results obtained for GPIT2.

The manus appears to allow significant digit extension (Fig. 5G, H, K, L). The distal condyles of the metacarpals are smoothly rounded trochleae, and there are small and shallow hyperextension pits visible on the distal ends of metacarpals II through IV. The phalanges show only very shallow or no hyperextension pits. Although the manus could certainly by used to support part of the animals weight, it does not show any special adaptations for a significant role in locomotion beyond the strong hyperextension of the digits. For example, the metacarpus is not elongated, and shows a significantly lesser development of inter-element contact surfaces, and thus stability, than the pes.

Hindlimb: hip.—Both hindlimbs of GPIT1 are preserved almost completely. The left pes lacks the distal tarsals and the ungual of digit IV, while the right hindlimb has large plaster replacements on the metatarsus as well as the phalanges. Therefore, a copy of the left tarsals, metatarsus and toes was used instead of the original right side elements. Most bones do not show any indications of significant deformations, except for the left fibula. This bone is damaged slightly below midshaft, and the remaining parts have been glued together in a slightly bent position. Overall, the left fibula is 1.7 cm shorter than the contralateral element. In the virtual skeletal mount it was positioned with the distal end correctly articulated with the tibia and the tarsals, therefore the proximal end is shifted distally compared to the tibia.

In the parasagittal plane, the femur can cover an angle of 65° without abduction (Fig. 6B), if retraction is assumed to end at the level of the ischia, and protraction before collision with the pubes. Further retraction may well have been possible, depending on the exact architecture of the m. caudofemoralis longus. However, resting positions are only feasible if the femora can be protracted at least 15° beyond the pubes (Fig. 6A, C, see below).

These limits on motion of the hindlimb in the parasagittal plane indicate that the long axis of the sacrum must have been held in a roughly horizontal position for speedy locomotion, as already concluded by Christian et al. (1996) and Christian and Preuschoft (1996). In a steep position as suggested for *Anchisaurus* by Marsh (1893a, b) and for *Plateosaurus* by Jaekel (1913–1914) and Huene (1907–1908, 1926), hardly any room is left for femur motions in the parasagittal plane, because the ischia approach a near-vertical position.

Adduction and abduction limits are difficult to determine. Bringing the foot under the body midline requires 15° of adduction, measured from the vertical (Fig. 6C), and abduction angles of as much as 45° may have been possible. Clearing the pubes at large protraction angles requires at least 22° of abduction (Fig. 6C). However, the missing cartilage in the hip joint does not allow an accurate assessment.

Hindlimb: knee.—The knee of *Plateosaurus* appears to be a simple hinge joint at first approximation, as in all extant taxa with parasagittal limbs. The exact degree of inversion and eversion possible cannot be determined due to the lack of preserved articular cartilage. The preserved bone shape of the distal femur end does not form a smooth continuous curvature in lateral aspect. Rather, there is a marked flattened part of the articular end, at a 110° angle to the long axis of the femur shaft. Assuming that this shape corresponds closely to the shape of the actual articular surface leads to the conclu-

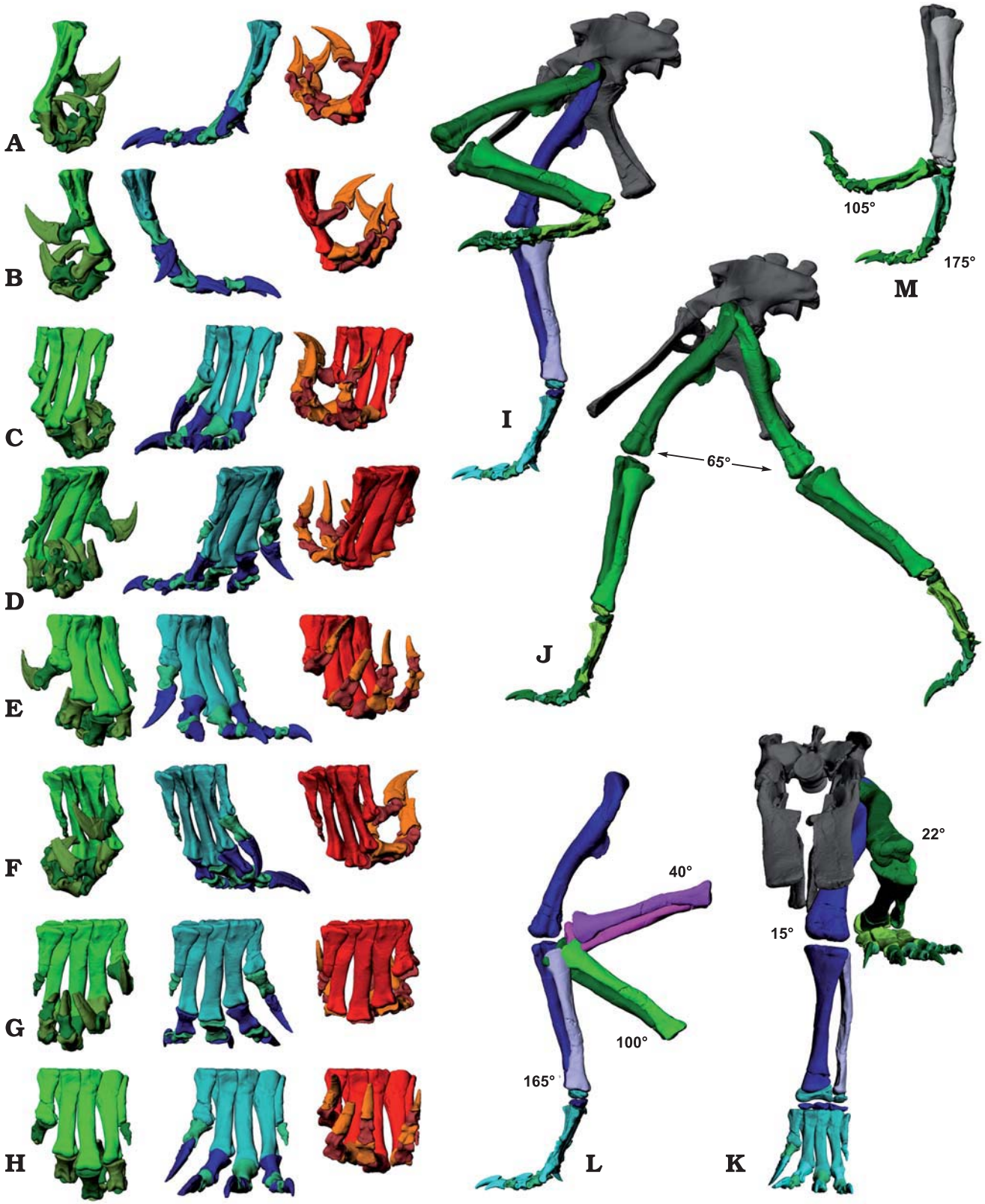

Fig. 6. Range of motion of the hind limb of prosauropod *Plateosaurus engelhardti* Meyer, 1837 using the digital skeleton mount of GPIT1, from Trossingen, Germany. **A**–**H**. Left pes in left to right: flexion, probable standing pose, extension, in lateral (**A**), medial (**B**), oblique (**C**–**F**), plantar (**G**), and dorsal (**H**) views. Length of metatarsal III 231 mm. **I**–**K**. Pelvis and left hind limb, in lateral (**I**, **J**) and anterior (**K**) views. I, K, probable standing (blue) and minimally possible flexion (resting) pose; J, maximum femur protraction and retraction angles for locomotion, resulting stride length 1.34 m. **L**. Left hind limb showing knee range of motion. Crus positions left to right: maximal extension, maximum flexion under large loads, maximum flexion for resting. **M**. Crus in lateral view, showing maximum ankle flexion and extension under load. Length of fibula 463 mm.

doi:10.4202/app.2009.0075

sion that there is a preferred articulation angle, in which the joint is positioned more stably than at neighboring flexion values, a sort of low-grade locking mechanism. However, this assumption is unreasonable for a joint that has to undergo rotation at a constant rate under loading, which is the case in the knee joint during locomotion. The distal condyles of the femur must therefore have been covered with a substantial amount of cartilage. Unless one assumes a cap that at its thickest point is 3 cm thick or more on the femur, there is no smooth curve possible over the distal end, and continuous extension and flexion under compression (i.e., during the stance phase of walking) would have been hindered by the "preferred orientation" of the joint. A similar bone and cartilage shape relation can be seen in juvenile and subadult extant birds, e.g., *Gallus domesticus* and *Struthio camelus* (own unpublished data), where the lateral aspect of the bony distal femoral condyles is also flattened, while the covering cartilage cap is well rounded distally. The tibiotarsus of *Gallus* also has a massive cartilage layer on the proximal end, similar in thickness to that of the femur. Here, however, the difference in shape between cartilage and bone is less pronounced, so that the bones give a good approximation of joint mobility.

A conservative estimate of the motion range is used here, based on the preserved surfaces and my own measurements and manipulations of *Gallus* knees. Maximum extension includes a 165° angle between the long axes of the shafts of the femur and the tibia, a maximum flexion angle of 100° under loading (e.g., during rapid locomotion), and a flexion to at least 40° without significant loading (e.g., in a resting pose) (Fig. 6D).

Hindlimb: ankle.—Like the knee, the intertarsal articulation allows motion mainly around the transverse axis. The main rotation occurs between the astragalus and calcaneum proximally, and the distal tarsals distally, as has been pointed out by Huene (1926). Only here exists a large convex/concave set of articulation surfaces that allows a continuous rotation over a large angle under load. The distal articular surface of the astragalus covers an angle of 170°. However, it appears unlikely that positions were possible in which the metatarsus is angled posteriorly in relation to the tibia, therefore the motion range can be reconstructed as covering angles between the long axis of the tibia shaft and the long axis of metatarsal 3 from 175° (maximum extension) to 105° (maximum flexion) under large loads (Fig. 6E). If no significant compressing force is active on the joint, flexion between the distal tarsal row and the metatarsus may have been possible, to facilitate the high flexion angles required for resting poses. However, feet preserved in articulation appear to achieve flexion to 130° (MSF 23), 22° (GPIT unnumbered, articulated hindlimb) or even 0° (SMNS F33) between the proximal and distal tarsals, without requiring tarsal/metatarsal motion. Obviously, these angles are affected by postmortem compression of the skeletons, but the fact remains that the limbs could be flexed to a resting pose with ankle flexion at values far below 90° between the astragalus/calcaneum and the distal tarsals alone.

Hindlimb: digits.—The range of flexion and hyperextension in the pedal digits is comparable to that in the manual digits (Fig. 6F–M). The claws of digits III and IV can touch the plantar surface of the metatarsus, while the second toe follows the same curvature path in lateral view, but cannot reach the metatarsus due to the smaller number of elements. The first digit has similar flexion mobility, too. As in the manus, it has a medially angled articulation between the metapodial element and the basal phalanx. Fully flexed, it curves laterally by 25° compared to the long axis of metatarsal III, which is a smaller angle than in the second digit (28°). Digit IV curves medially by 14°.

A telling detail for the interpretation of the manus and pes function is the slight difference in shape of the distal ends of the metatarsals and metacarpals II through IV. In the manus, the distal articular condyles are significantly wider ventrally than dorsally, while in the pes the ventral and dorsal transverse extent is subequal in digits II and III. This indicates that the main forces acting on these articulation occurred during flexion in the hand, while there is no clear preference in the pes. This pattern is not compatible with quadrupedal locomotion. Additionally, in contrast to the knee and the metacarpal/basal phalanx articulations, the metatarsal/basal phalanx joints have a preferred articulation angle. A flattened area of the distal articular end is orientated at roughly 70° to the long axis of the metatarsus on metatarsals II through IV. In contrast to the knee, there is no indication that significant amounts of articular cartilage are missing. Rather, the articulation surfaces are well ossified. Articulating the basal phalanges with the metatarsus to achieve maximum bony contact results in a position conformal to a high digitigrade stance. The basal phalanges create the shift from subvertical to horizontal, and the distal ends of the metatarsals are lifted off the ground (Fig. 6A, D). Under high compressive loads, e.g., when taking up the weight of the animal during rapid locomotion, or on soft substrates, the distal ends of the metatarsals probably contacted the ground. The proximal surfaces of the basal digits are shaped to conform to the flattened area of the metatarsals, creating a weak locking mechanism. If the joint is compressed during the support phase, rotating or sliding motion away from the preferred articulation angle results in intra-joint forces that favor the preferred angle. A similar, though more elaborate structure is present in the wrists of ungulates, where roughly cubic carpals lock the joint in a straight position under pressure, but allow strong flexion (two times to 88°) for folding the manus under the antebrachium when the animal lies down.

In digit IV, the distal end of the metatarsal has a medial condyle that is equally sized dorsally and ventrally, while the lateral condyle is limited to the ventral face (differing from the other two long pedal digits). Dorsally, there is a pronounced gap, leaving the dorsolateral edge of the proximal articulation surface of the basal phalanx (indistinguishable in shape from

those of digits II and III) free of an immediate bony contact. The functional significance of this feature is unclear.

Mobility of the complete skeleton

For the creation of a complete skeletal mount, most skeleton parts were easily combined, e.g., the tail and the sacrum. However, taphonomic damage to the first sacral has tilted the anterior surface of the centrum as well as the neural arch backwards by an unknown amount. Therefore, the prezygapophyses have been displaced caudally, and their correct orientation cannot be ascertained, making alignment of the dorsal and sacral series difficult. Most other sacra of *Plateosaurus* are also damaged (Moser 2003; own observation), but in general the first sacral has roughly parallel caudal and cranial faces of the centrum, and the center of the prezygapophysal articulation surface rests directly dorsal to the cranial face of the centrum. The virtual skeleton was mounted accordingly, causing a wedge shaped gap between the last presacral and the first sacral. The resulting continuous curvature of the vertebral column across the dorsal/sacral transition is further indication that this arrangement is correct.

Fig. 5A–E and SOM 1 (http://app.pan.pl/SOM/app55-Mallison_SOM.pdf) show the full motion range of the complete forelimb. Fig. 6B, D, E and SOM 2 (http://app.pan.pl/SOM/app55-Mallison_SOM.pdf) show the motion range of the hindlimb available for locomotion, without strong femur abduction, while Fig. 6A, C depict maximum limb flexion.

Aside from neutral pose, various flexion/extension combinations were created to assess the overall mobility of the animal. The aim was not to demonstrate the possible extremes of motion, but rather functional poses, such as resting poses, or a pose that brings the head to the ground, e.g., for drinking or feeding. These occasionally highlighted collisions between body parts, limiting overall range of motion. When the dorsal series is ventrally flexed, the distal ends of the posterior ribs quickly reach the level of the pubes, at flexion angles of below 5° in each of the last four intervertebral articulations. While some overlap may have been possible, further ventriflexion compresses the digestive tract to an improbable degree. Similarly, large adduction angles combined with large retraction angles place the distal end of the humeri within the ribcage.

Ground feeding.—One pose (Fig. 7A) was created to show how the "stepping up" of the neck caused by the trapezoidal cervical centra affects the animal's ability to bring the snout to the ground, e.g., for drinking to feeding. Huene (1928) suggests that *Plateosaurus* had to perform a see-saw motion in the hips, but that is apparently based on the assumption that the back is not sub-horizontal in the habitual standing posture. In fact, from a pose with a horizontal back and nearly straight hindlimbs, a bending of the anterior half of the thoracic vertebral column, combined with a slight increase in limb flexion and maximum ventriflexion of the neck suffices to bring the snout to the ground. The hands are almost able to reach the ground in this position.

Manus at ground level.—Grasping objects at ground level with the manus requires slightly more flexion of the vertebral column, or a slight downward rotation at the hip. In this position the head can reach significantly below ground level (Fig. 7B).

Resting.—The resting pose of *Plateosaurus* (Fig. 7C, D, SOM 3 at http://app.pan.pl/SOM/app55-Mallison_SOM.pdf) follows the position of the articulated finds, and that of SMNS F33 especially. Jaekel (1913–1914) assumed that *Plateosaurus* habitually rested on the distal ends of the ischia. Such a posture is possible (Fig. 6C, D), but requires extreme flexion of the hindlimbs. Resting on the pubis, as is known from theropods (e.g., Gierlinski et al. 2005; Stevens et al. 2008) is not possible, and there is no enlarged pubic foot. The pelvic girdle in the tight articulation and low position chosen here and in Mallison (2010) partly supports the weight of the anterior body, so that the ribcage is not compressed.

Previous reconstructions

Skeletal mounts.—The GPIT1 mount in the IFGT (Fig. 1D) is mostly correctly articulated and placed in a plausible bipedal pose with slightly flexed hindlimbs. Solely the massive splaying of the metacarpals and the slight splaying of the metatarsals are unrealistic. GPIT2 is similarly well articulated, also has splayed metapodia, but is posed in a possible, but not plausible posture. The animal appears to be running quickly, but the back is angled steeply, so that the femur of the supporting limb is already retracted close to the ischia although the limb is roughly vertical. The other limb is lifted clear off the ground with a strongly flexed knee and ankle. While *Plateosaurus* certainly could adopt a pose with a steeply inclined back, it would have severely hampered limb retraction, and thus rapid locomotion. Therefore, the animal should have both feet on the ground, as the pose is more suited for high browsing than for running. Similarly, AMNH 6810 (Fig. 1F) is mounted in correct articulation, but for a slight splaying of the metacarpals and metatarsals. The pose is overall quite similar to the head-to-ground pose in Fig. 6A, but he tail is drooping. The old MFN mount of skeleton C (MB.R.4430.1–4430.12) by Otto Jaekel was also placed in a pose that was possible, but not necessarily plausible. Notably, it was the only mount that did not disarticulate any bones.

All old SMNS mounts shared a series of errors that can still be seen in the remaining quadrupedal mount (Fig. 1G). The ribcage is bloated to create a broad oval, reminiscent of a lizard, tilting the scapulae so that the glenoids face anterolaterally (with correctly articulated, medially touching coracoids). The proximal end of the humerus is placed lateral to the scapulacoracoid, so that compressive forces on the forelimbs would shear the humerus from the glenoid. Despite the semi-sprawling posture, the frontlimbs do not allow sufficient manus pronation to make the palm face the ground with

doi:10.4202/app.2009.0075

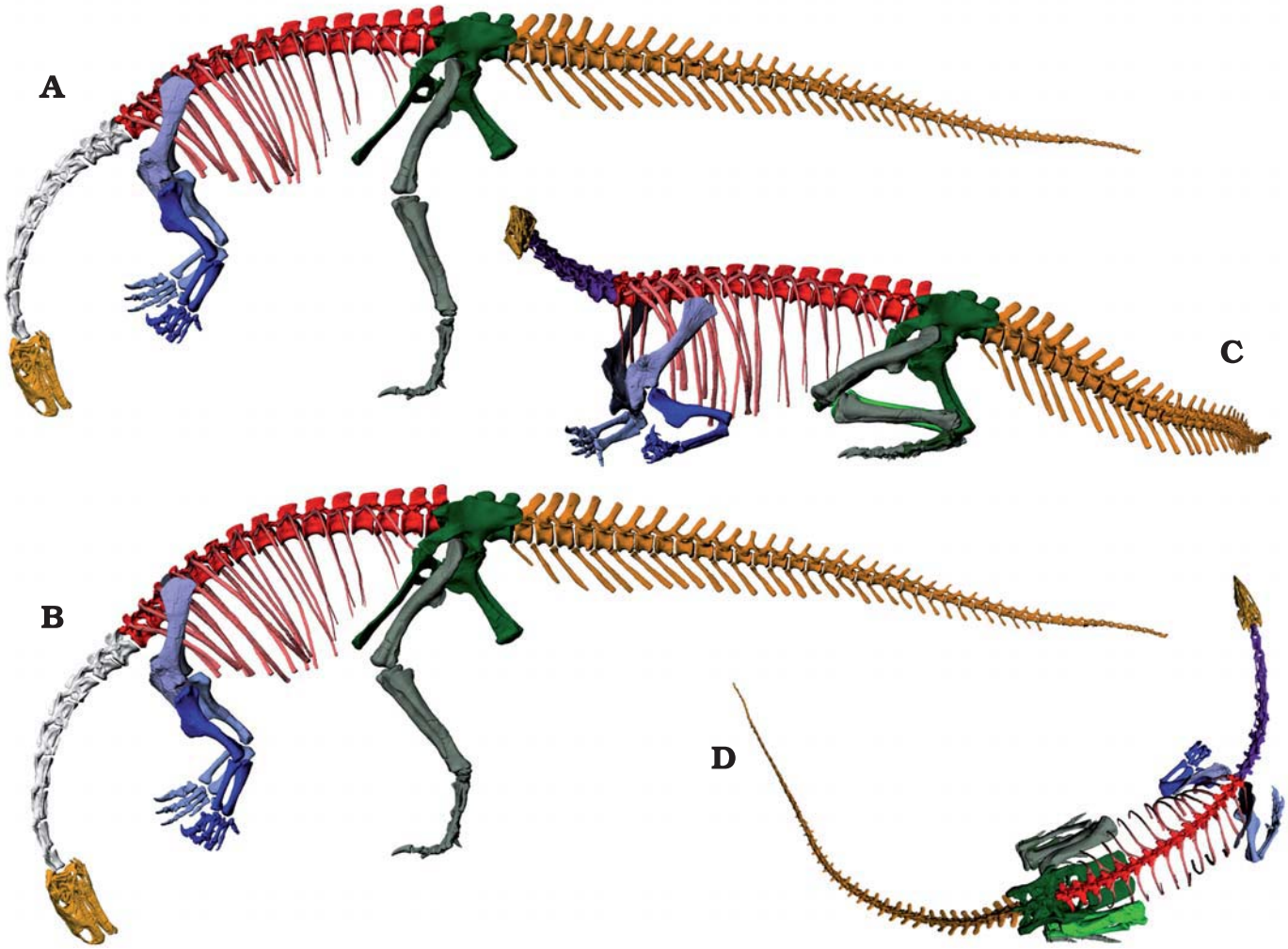

Fig. 7. Digital skeleton mount of prosauropod *Plateosaurus engelhardti* Meyer, 1837 GPIT1, from Trossingen, Germany, posed: head at ground level (**A**), hands at ground level (**B**), resting pose in lateral (**C**) and dorsal (**D**) views. Length of femur 595 mm.

the digits pointing cranially. Therefore radius and ulna have exchanged position in the articulation with the humerus, a condition totally unknown in any extant taxon, even in birds, where the radius lies anteriorly, not medially, of the ulna. The track in the forelimbs is wider than their stride length. Also, the anterior ribs are arranged at a right angle to the vertebral column. That this is incorrect is immediately obvious on the mounts, because the gastral basket reaches only as far forward as the fourth rib, creating a large gap between the coracoids and the first gastralia. In life, the sternals would have been situated in this gap, but are of insufficient size to fill it (Huene 1926). If the animal rested on the ground, this arrangement would mean that the anterior ribcage would not have been protected from dorsoventral compression in any way, while correct articulation leads to the coracoids and sternals serving as a resting surface, transferring forces to the scapulae and thus protecting the thorax. As a direct result of the extremely wide ribcage, the femora have to be abducted widely as well. This creates the need to angle the lower limb strongly inwards in relation to the femur, causing a wedge-shaped gap in the knee. The resulting overall proportions and limb positions are in direct contradiction to the adaptations to cursoriality visible in *Plateosaurus*, and require significant disarticulation in several parts of the skeleton.

In addition to these general inaccuracies, one now dismantled mount (SMNS 13200 cast) set up in a bipedal running posture exhibited a special problem. The foot in stance phase was placed ~0.5 m laterally of the midline, with the femur abducted instead of adducted. Running with abducted limbs requires strong transverse motions, which is energetically very inefficient. Such behavior is advantageous solely for creating larger body velocities per traveled distance than running without swaying, which is why human athletes sometimes use such a run for the first few steps of a run-up. For flight, e.g., from a predator, it is disadvantageous.

The mount in the BSGP, the creation of which is described in detail by Moser (2003), is well articulated except for the pectoral girdle and forelimbs. As in the SMNS mounts, the radius and ulna are exchanged, resulting in manus pronation. The ribs are angled too far forward, increasing the thorax volume. Additionally, the pectoral girdle is widely separated along the midline, causing an artificially

wide shoulder area. The metacarpals and manual digits are widely splayed. The pedal digits curve strongly medially. This track has digit proportions that are incompatible with *Plateosaurus*, as described by Moser (2003). The reason for this misalignment is clearly stated in Moser (2003: 146): "the limbs were for the first time mounted according to the template of a scaled quadrupedal trackway of a prosauropod into the exactly predefined distances, so that the forelimbs are further abducted than the closer and more vertically placed hindlimbs" (translation from the German by the author). This adherence to a certain trackway also induces a lateral curvature into the dorsal vertebral column.

Reconstruction drawings.—The oldest reconstruction drawing by Jaekel (1913–1914: pl. 4; Fig. 2C) was created with the knowledge of complete and partial skeletons found in articulation. Surprisingly, the overall proportions are incorrect, with the neck significantly too short, the humeri increased to nearly 130% original size, the rest of the forelimb scaled by ~115%, the femur lengthened by 40%, and the antepodium and metapodium as well as the pedal digits scaled to 120%. These values are probably too low for humerus and femur, because Jaekel (1913–1914) assumed a sprawled position, so that perspective shortening is present in his drawing, but not in the digital mount. As a direct result, the proximal head of the femur is at least as wide as the acetabulum, leaving no room for cartilage at all. The pattern of scaling errors is inconsistent with a simple mistake, such as an accidental size increase in all limb elements. Rather, the proximal elements are enlarged more than the distal parts, and the neck is too short, giving the animal a much stouter and clumsier look than a correctly proportioned reconstruction. Interestingly, Jaekel's reconstruction drawing of the complete animal (Jaekel 1913–1914: pl. 4) has the same neck/trunk proportions as his figure of the presacral vertebral column (Jaekel 1913–1914: fig. 15), with the neck roughly 67% the length of the dorsal series, while summing the length of the centra as given by Jaekel (1913–1914: 181–182) results in a ratio of 85%, similar to SMNS13200, GPIT1 and GPIT2. Also, the reconstruction drawing separates radius and ulna widely, so that their proximal ends articulate with the lateral side of the lateral and the medial side of the medial condyle, while Jaekel (1913–1914: fig. 18) depicts them tightly placed as found in situ.

Three other reconstruction drawings are very similar to each other and will be discussed together. These are those of Huene (1926; Fig. 2B), Weishampel and Westphal (1986; Fig. 2F), and Galton (1990; Fig. 2E). They have in common that the overall proportions of the animal, as well as those of all larger bones, conform to SMNS13200. None appears to correct for the deformation of the sacrum, so that the pelvic girdle and hindlimbs are shifted posteriorly compared to the rest of the skeleton by approximately the length of one sacral centrum. Bone proportions vary slightly between the different drawings, as is to be expected when drawings are created manually, and not in a computer program. In general terms, however, they are correct. Because Galton's (1990) drawing is explicitly based on Huene (1926), the commonalities between them are to be expected. In all three drawings the manus looks clumsy, because of an almost radial splaying of the metacarpals.

Paul (1987, 1997, 2000; Fig. 2A) offers the only dorsal and anterior/posterior views of *Plateosaurus*. The virtual skeleton was first arranged to conform to the lateral view alone, highlighting a series of significant problems. In order to determine which of the discrepancies are caused by intraspecific variation, the drawing by Paul (1987) was also compared digitally to the drawings of the articulated neck and tail and the separate limb bones from Huene (1926: pls. 1–4), and especially to Huene (1932: pls. 26–29), on which it was based (Paul 1987: 29). In all bones, the proportions of Paul's (1987) drawing are exactly those of MB.R.4402 (Huene 1932: pls. 26–29, there listed as Fund 25). Several bones are not shown in lateral view in Huene (1932), e.g., the femur and humerus. Whether Paul (1987) based his drawing on figures of other individuals of *Plateosaurus* in Huene 1932 is unclear. Radius and ulna are depicted in later view in Huene (1932), and thus copied in Paul (1987). Why Paul (1987, 1997, 2000) assumes a sigmoidal curvature of the radius shaft that allows pronation, as evident from his drawings, is unclear. Placing the digital skeleton to conform to Paul's (1987, 1997, 2000) drawings results in a total disarticulation of the wrist (Fig. 8A, B). An additional erroneous articulation is evident in the first manual digit. Both metacarpal 1 and the phalanges of digit I are figured in detail by Huene (1932: pl. 28: 6, 9, 10). Paul (2000) assumes a 90° angling between the ungual and the metacarpal, although there is no evidence of anything but a slight medial angling because of the unequal distal ginglymus of metacarpal I in Huene's (1932) figures.

The right hindlimb is protracted significantly forward of the pubes, which have been rotated slightly backwards (Figs. 2A, 8D, E). The right ankle is hidden from view by the left antepodium. To match the visible parts, the distal tarsals and proximal end of the metatarsus must penetrate the proximal tarsals and distal ends of tibia and fibula (Fig. 8C). Correcting this error results in a position in which the claws touch the ground, a pose unsuitable for limb protraction during locomotion. Lifting the leg higher up requires either even further extension of the ankle, or further protraction of the femur. Both options are difficult, because the ankle is already quite extended, and the femur is already unrealistically protracted beyond the level of the pubes.

The anterior view of the pectoral girdle and forelimb in Paul (1987; Fig. 2A) is combined with a posterior view of the pelvis and hindlimb. Aligning the scapulae shows that Paul (1987) assumes massive rotation to take place, and has misplaced the clavicles (Huene 1926; see also Yates and Vasconcelos 2005 on the pectoral girdle of *Massospondylus*). In the anterior view, radius and ulna are shown in a crossed position, allowing the wrist to remain articulated, but creating an intersection between the bone shafts. The problematic articulation of the first digit mentioned for the lateral view becomes evident, too (Fig. 8B). Additionally, while the left limb is placed under the center of mass, the protracting right limb is

doi:10.4202/app.2009.0075

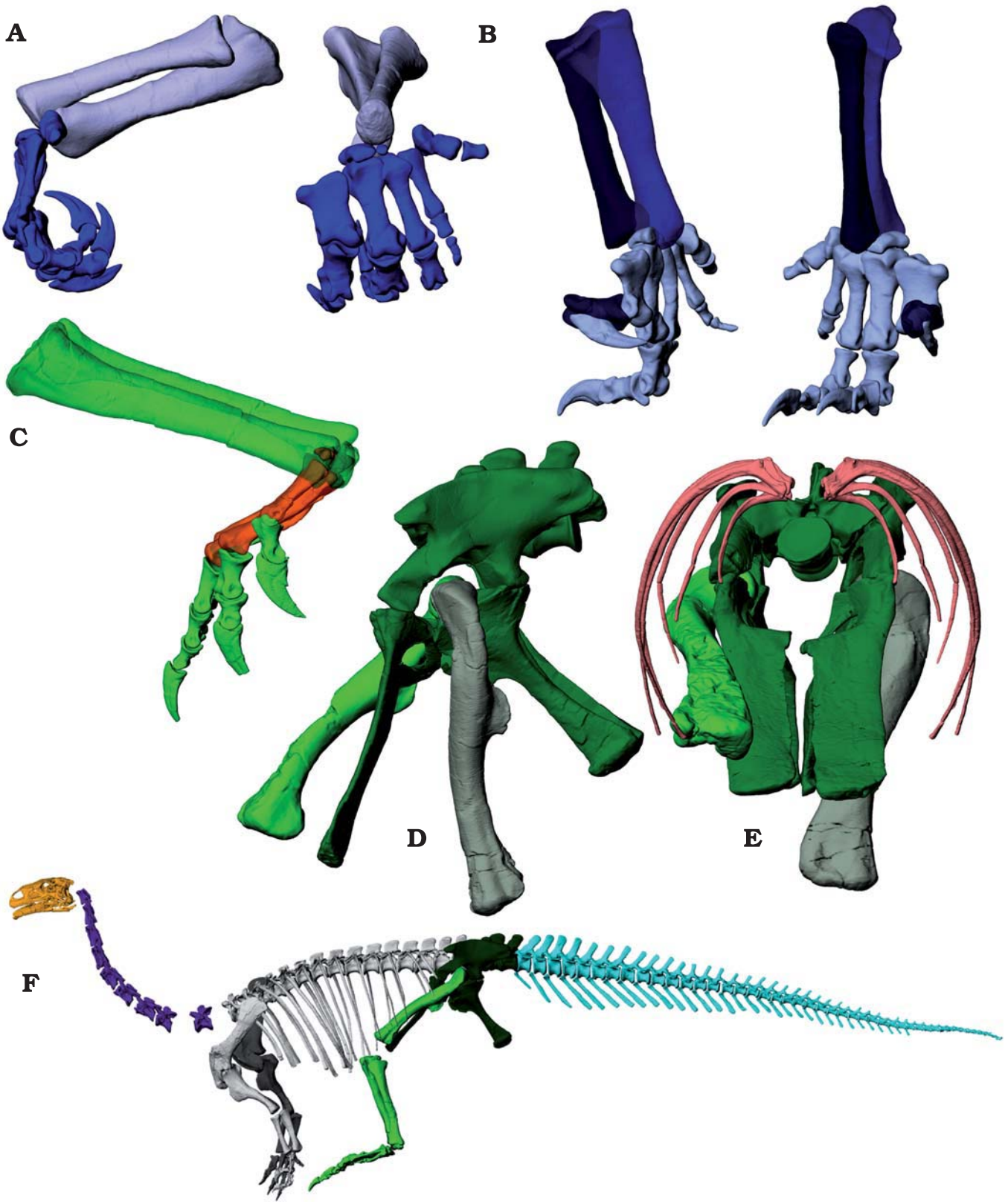

Fig. 8. Digital skeleton mount of prosauropod *Plateosaurus engelhardti* Meyer, 1837 GPIT1, from Trossingen, Germany, posed to conform to drawings by Paul (1987, 2000; Fig. 2A). **A**. Left antepodium and manus in lateral and dorsal view. **B**. Right antepodium and manus in medial and dorsal view. **C**. Right crus and pes in medial view. Note intersection of tarsals and metatarsals with crus. **D**. Pelvis and femora in lateral view. **E**. Anteroventral view, parallel with the long axis of the dorsal column, of the pelvis and femora and the last five dorsal ribs. **F**. Lateral view of "gallop" position. Note gaps in knees and neck. Length of ulna 239 mm, length of fibula 463 mm, length of femur 595 mm.

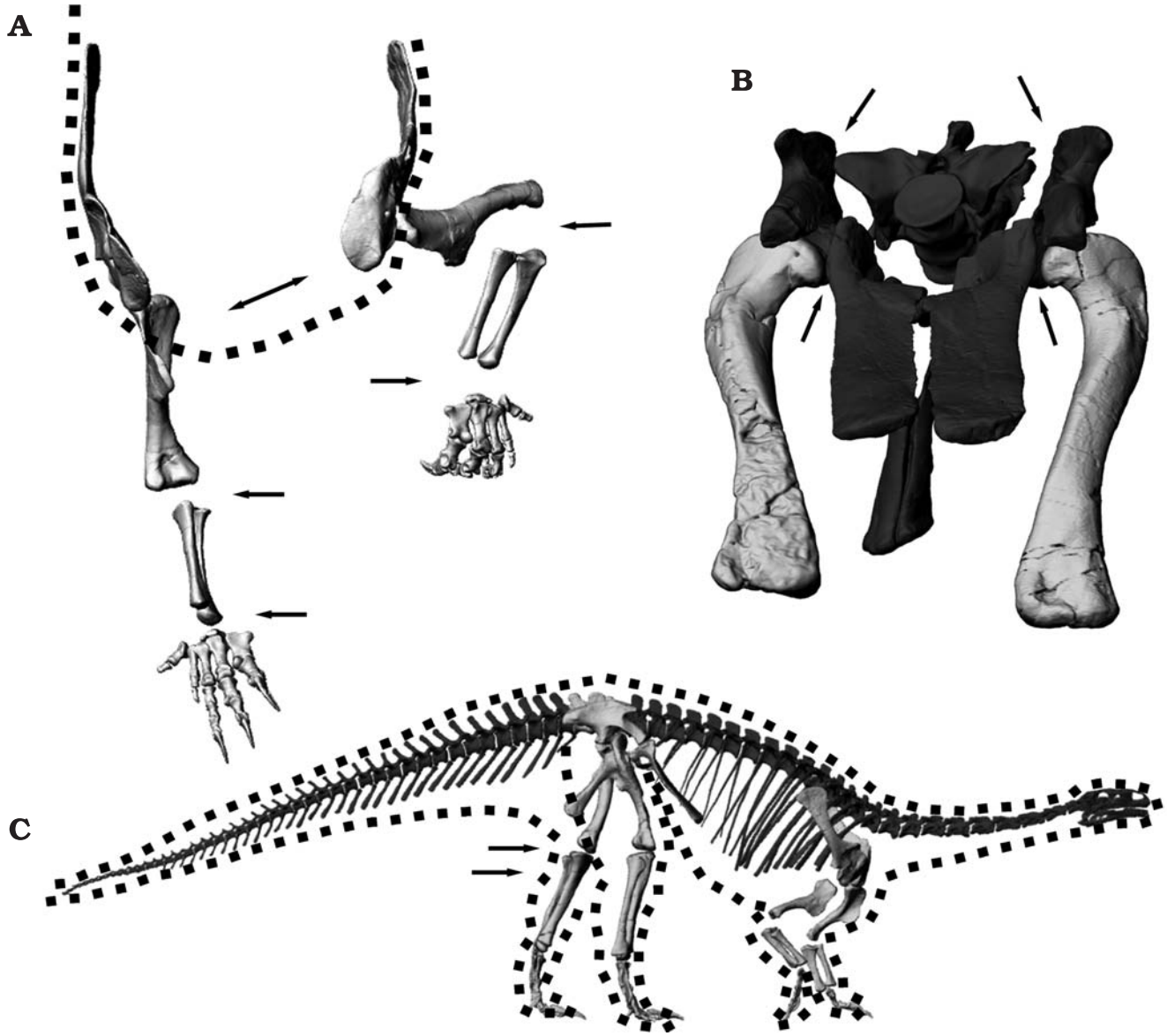

Fig. 9. Digital skeleton mount of prosauropod *Plateosaurus engelhardti* Meyer, 1837 GPIT1, from Trossingen, Germany. **A**. Anterior view of the pectoral girdle and forelimbs posed to conform to the life-sized, bipedal SMNS model (Fig. 1J) of *Plateosaurus engelhardti*. Dotted line indicates body outline of the model. Note gaps in elbows and wrists and too large gap between coracoids (arrows). **B**. Anterior view of the pelvic girdle posed to conform to the life-sized, bipedal SMNS model (Fig. 1J). Note gaps in the pelvis between sacrum and ilia, and between ilia and pubes (arrows). **C**. Virtual skeleton posed to conform to the toy model version (Fig. 1L) of the new SMNS quadrupedal model (Fig. 1K, L) of *Plateosaurus engelhardti*. Dotted line indicates body outline of the model. Arrows mark skeleton's (upper) and model's (lower arrow) knee joint. Note gaps in forelimbs and posterior ribs extending below the pubes. Length of the femur 595 mm, length of the ulna 239 mm.

abducted in the dorsal view, however, not to a sufficient degree to clear the (incorrectly reconstructed) ribcage (Fig. 8E). Alternatively, it is possible that the femur is abducted in the lateral view drawing, but the perspective shortening insufficiently taken into account. Also evident in Paul's (1987) drawing is an inward cant of the shank in the supporting limb, which would open a wegde-shaped gap in the knee.

Paul's (2000) reconstruction of the animal in a gallop shows massive scaling inaccuracies, as the neck, trunk and thigh are too long (Fig. 8A). Additionally, both femora appear to be protracted without massive abduction to beyond the level of the pubes, because there is no perspective shortening of thigh, shank or foot visible. It is unreasonable to assume that *Plateosaurus* could move in this fashion at all, because limb extension in the hindlimb would require large muscle moment arms around the ankle and knee, while the corresponding osteological features suggest small moment arms (no pronounced cnemial crest, no tuber calcanei).

The inaccuracies concerning the tail curvature in the drawing by Wellnhofer (1994; Fig. 2D) have already been pointed out in detail by Moser (2003). Except for a significantly too large coracoid, the proportions of Wellnhofer's (1994) drawing are correct. However, the manus is pronated, and the dorsal ribs are misaligned.

doi:10.4202/app.2009.0075

Comparison of Hartmann's reconstruction (Fig. 2G; www.skeletaldrawing.com) to the virtual skeleton mount of GPIT1 reveals no significant differences. The metatarsi are slightly shorter in the drawing, but otherwise proportions, articulation angles and body outline match well.

Life-sized and digital models.—The old life-sized SMNS models were based on the skeletal mounts and share their errors in proportions. Most notable are the hands and feet, which are about double the width they should be. Also, the knee was shifted distally by about 0.2 m. The new SMNS models, created under the direction of Markus Moser, all show the incorrectly wide pectoral region of the BSPG mount (see Moser 2003). Additionally, the pelvis appears wider (Fig. 9B; compare to correct articulation in Figs. 6C) and the forelimbs longer than they should be (Fig. 9C; note the gaps in the elbows). The knee is shifted about 0.1 m distally (Fig. 9C). The manus and pedes have short digits, strongly medially rotated as in the BSGP skeletal mount. Apparently, the models are also supposed to conform to the trackway mentioned in Moser 2003.

The fat 3D digital model of Gunga et al. (2007) is decidedly too muscular, especially in the neck and trunk, and has feet much bigger than the skeleton. Additionally, the feet are simplified so that the spaces between the digits are filled with matter, further increasing their weight. These errors are evident in Gunga et al. (2007: fig. 3b). The slim model of Gunga et al. (2007) has a more realistic body outline, although some details are questionable. For example, the limb diameters do not correlate to expected muscle volumes, so that the crus is widest at the midshaft of the tibia, not near the proximal end.

Discussion

Range of motion.—Combining the data detailed above results in a reconstruction of *Plateosaurus engelhardti* (GPIT1) as a surprisingly slender (for a herbivore) biped, with a subhorizontal back and tail position (Fig. 1E; Mallison 2010: fig. 1.2), strong grasping arms with a limited motion range, and the ability to obtain a 360° view by small head and neck motions alone.

The vertebral column in *Plateosaurus* exhibits no surprising specializations. In contrast to more derived sauropodomorphs (Apesteguia 2005), there is no hyposphene-hypantrum articulation present that could block lateral motions. The dorsal series allows significantly more mobility between neighboring vertebrae than can be used when the ribcage is taken into account. This may allow decoupling of the main mass of the body from the dorsoventral accelerations that the pelvis will experience during rapid locomotion, reducing the need to avoid such motions through increased limb flexion at midstance.

Reconstructing the resting position of *Plateosaurus* (Fig. 7C, D) based on articulated fossils shows clearly that the articular ends of the limb bones as preserved are not a reliable indicator of the shape of the articular surface in life. The bone shapes suggest a maximal flexion angle to nearly 90°, but any reasonable resting position requires at least 45° more. This confirms that the longbone ends as usually preserved in dinosaurs are not a reliable indicator for the shape of the articulation surface, as above shown for the ulna of *Kentrosaurus* (Fig. 3B, C).

The pes of *Plateosaurus*, with only digit 5 significantly reduced and a marked grasping ability (Fig. 4L), can be interpreted as an adaptation to scratch digging, potentially for scooping out nests. In comparison to other bipedal dinosaurs, the motion range of the forelimbs of *Plateosaurus* is remarkably primitive. As in the basal theropods elbow flexion is limited (Senter 2006b). Similarly, humeral elevation and protraction are possible to a much lower degree than in even basal members of the Avetheropoda (Senter 2006a), and similar to the carnosaur *Acrocanthosaurus* (Senter and Robins 2005). This limited the range to below and barely laterally of the body. One-handed grasping of small objects was possible (Fig. 5G–J), as well as holding and manipulation of larger objects with both hands. Handling objects or feeding at ground level was possible in a pose that did not inhibit rapid flight, and did not require support by the forelimbs (Fig. 7A, B). The claws were probably not sharp and curved enough to allow grasping or penetrating objects with them alone, in contrast to most theropods. This reinforces the notion (e.g., Galton 1984, 1986b) that *Plateosaurus* was not a carnivore as suggested by Cooper (1981), but a herbivore. It cannot be determined, due to the uncertainties regarding neck mobility, whether the snout could be brought into contact with the hands. Recently, a pair of clear theropod manus imprints were found as part of a longer trackway that indicates either a habitual manus posture with medially directed palms, or an inability of theropods to pronate the manus any further (Milner et al. 2009). Together with the only partly pronated manus of stem-sauropods (Remes 2008) this raises the question of whether any early sauropodomorph was able to pronate the manus fully. Medially directed palms and the inability to pronate the manus may be ancestral characters, calling into question the assignment of quadrupedal tracks with a narrow gauge in the frontlimbs to sauropodomorph dinosaurs. Alternatively, strong undulation of the anterior body must be assumed.

The estimated tidal volume of GPIT1 of 20 liters as determined from rib motion (Fig. 4F) corresponds to ~29 ml per kg body weight for the average body mass of GPIT1, estimated by Mallison (2010) as 690 kg. This value is within the spread of extant birds, close to those of *Anser* (*Anser anser* 31.4 ml/kg, *Anser indicus* 28.26 ml/kg, values calculated from data in Frappell et al. 2001: table 1), and significantly different from the average value of terrestrial mammals of ~7.7 ml/kg (Stahl 1967). Among mammals, tidal volumes around 22 ml/kg are typical for marine forms (Mortola and Seguin 2009). This indicates that *Plateosaurus* possessed a high performance lung comparable to extant birds. The minimal tracheal volume of *Plateosaurus* can be estimated at slightly over 360 cm^3, based on an airway length of 1.30 m, and an estimated diameter of 6 cm, which corresponds to 5

cm^3/kg bodyweight. This value is similar to the value found in an ostrich (*Struthio camelus*: 6.13 cm^3/kg, data from Maina and Nathaniel 2001).

The sister group to Sauropodomorpha in Saurischia, Theropoda, possessed osteological correlates to flow-through ventilation adaptations in all but the most basal forms (O'Connor and Claessens 2005). Recently, unidirectional airflow has also been found in alligators (Farmer and Sanders 2010). *Plateosaurus*, like all prosauropods, lacks unequivocal evidence for postcranial pneumaticity (Wedel 2007). However, several lines of evidence suggest that lung ventilation via air-sacs is a primitive character of Saurischia as a whole (Wedel 2009). The lack of invasive pneumatic foramina in the dorsal vertebrae does not exclude the possibility that the lungs were attached there (Perry 2001). The cervicals also lack invasive pneumatic foramina, the only unequivocal evidence for postcranial skeletal pneumaticity, which would indicate the presence of air sacs (Wedel 2003, 2007). However, the centra of the last five cervicals show deep recesses under the transverse processes, which may in life have been filled by non-invasive cervical air sacs. The close correspondence of the tidal volume per mass determined here further reinforces this notion.

Previous reconstructions.—The reconstruction drawing by Jaekel (1913–1914: pl. 4) suffers greatly from a preconceived notion: that *Plateosaurus* had a lizard-like sprawling posture. Jaekel (1913–1914: 190) also assumes plantigrady, because of the existence of large curved pedal claws, and copies inexact proportions from one of his figures into the reconstruction. Jaekel (1913–1914) also mentions repeatedly that his interpretation is greatly influenced by the position of the skeletons as found in the field, ignoring the fact that this pose may not be a habitual pose, may be influenced by post-mortem deformation, or may be habitual as a resting pose only.

The reconstructions of Galton (1990) and Weishampel and Westphal (1986) greatly resemble that of Huene (1926). All three reconstructions are classic depictions of the general osteology of the figured species, and give a good impression of the animal's overall shape.

In contrast, the drawings by Paul (1987, 1997, 2000) contain a number of inaccuracies (Fig. 8) that are a direct contradiction of the detailed description in the text and figures in Huene (1926), and even to the figures in Huene (1932), on which they were based. Paul's (1987, 1997, 2000) drawings clearly are not based on a three-dimensional understanding of the bone articulations, as evident by the protraction of the femur far beyond the level of the pubes without the required massive abduction (Fig. 8E), which should be evident in both lateral and dorsal views, by the misplacement of the clavicles on the dorsal rim of coracoids and scapulae, by the rotation of the scapulae against each other, and by the total disarticulation of the antebrachium introduced by enforced manus pronation (Fig. 8A, B). Even more surprising is the clearly sigmoid curvature of the radius shaft and the apparent 90° rotation between the long axes of the proximal and distal articular ends of the radius in the anterior view (Paul 2000; Fig. 2A), in direct contradiction to Huene (1932: pl. 28). These and other errors cannot be explained simply by the fact that Paul (1987: 49) did not inspect the actual fossils, but based his reconstruction on the drawings from Huene (1932) alone. Rather, the errors seem to result from a preconceived notion that prosauropods were quadrupedal, that their manual digits I were raised off the ground during locomotion (following Galton 1971a, b; Weems 2003), and a desire to depict the animal in as dynamic a pose as possible. This is especially true for the 90° medial angling of the first manual ungual, which is in direct contradiction to the figures in Huene (1932), as well as the massive errors in proportion in the right hindlimb of the skeletal outline drawing (Fig. 8C) and the left hindlimb of the "galloping" drawing (Fig. 8F). It must be mentioned that Paul (2000: 78), writing about restoring the life appearance of dinosaurs, stated: "A high-quality life reconstruction begins with a good skeletal reconstruction. Restorations based on previously published skeletal restorations or outline skeletal sketches usually prove to be seriously flawed. Also important are multiple-view restorations of at least one representative of each major group. These make obvious anatomical errors not always apparent in side view, and they detail the subject's three-dimensional structure". Paul (1987, 1997, 2000) highlights with his reconstruction drawings of *Plateosaurus* that even the mentioned multi-view restorations are insufficient to make anatomical errors obvious, or to detail the 3D structure of the animal.

Museum mounts and models appear to suffer similarly from preconceived notions. The old SMNS mounts (Fig. 1G, H) are highly inaccurate in comparison with the virtual skeleton of GPIT1, considering the opportunity their creators had of manually manipulating casts of SMNS 13200 before mounting them. The underlying cause of almost all problems in the old SMNS mounts is the decision that *Plateosaurus* must be a "typical reptile", which is a marked contrast to the generally accepted and well supported view that dinosaur and lizard locomotion were fundamentally different (e.g., Bakker 1986). The decision that *Plateosaurus* must also have been able to feed in an upright pose, combined probably with a misjudgement of the position of the center of mass due to the artificially enlarged body cavity, forced the awkward-looking dorsal curvature in the posterior dorsals of the upright mount (Ziegler 1988: cover illustration, fig. 4; Moser 2003: fig. 4), when in fact a bipedal, high-browsing pose is easily feasible with a nearly straight dorsal series. The old, upright 3D life-sized (Fig. 1C) and toy models suffer from the same problems, as evident from comparison of both photographs and the digitized toy model to GPIT1.

The *Plateosaurus* mount in the BSPG was clearly planned a priori as a quadrupedal mount, based on the trackways mentioned by Moser (2003). The wide track of the forelimbs and the undulating vertebral column create the impression of a crocodile in a high walk, albeit with an even slightly wider forelimb posture. Here, the direct evidence from the bones was ignored in favor of the at best question-

doi:10.4202/app.2009.0075

able assignment of an ichnotaxon to an unspecified "prosauropod", despite the uncertainty involved in the assignment (which Moser [2003] explicitly mentioned) and the diversity evident within "Prosauropoda". The new SMNS 3D models were created so that the quadrupedal model would fit the same trackway as the BSPG skeletal mount (Markus Moser personal communication 2004). The change of placement of the knee evident in at least one model (Fig. 9C) together with the sauropod-like feet (Fig. 1J–L) hides the extreme contrast between the short, sturdy forelimbs and the long and slender hindlimbs. These inaccuracies in the model illustrate that the skeletal evidence was ignored in favor of a desired goal.

The mount of *Plateosaurus* in the MFN articulated the entire skeleton correctly, although the pose chosen by Jaekel was certainly not a habitual posture of *Plateosaurus* (contra Jaekel 1913–1914). It deserves special mention that this was the sole mount discussed here that contained no significant incorrect articulation between any neighboring bones, within technical limits (i.e., contained no disarticulation, except for a slight splaying of the left, but not right, metacarpals). The plantigrade, tail-dragging posture is well within the possible motion range of *Plateosaurus*, e.g., for upright feeding, although the highly flexed hindlimbs would make sustaining the pose for an extended time rather exhausting.

In summary, it becomes apparent that preconceptions are the greatest source of errors in reconstructions of extinct animals. Similarly damaging to the final result is a lack of experience in articulating bones correctly, either from a lack of anatomical knowledge, or from neglect to attempt manual articulation of the bones. Many errors, especially the exchanged antepodial elements in skeletal mounts (Fig. 1G), could have been avoided with a few simple attempts to manually articulate the elements correctly before an armature was created, and an extant phylogenetic bracket (Witmer 1995) comparison. Adapting previously published data without keeping its limitations in mind, e.g., using small-scale drawings to create new reconstructions in a different pose, carries a high risk of misunderstanding the 3D articulation of bones, leading to significant errors and thus incorrect biomechanical and paleobiological interpretations.

The optimal way of creating a skeletal mount is thus the manual (e.g., Senter and Robins 2005) and/or digital (e.g., Mallison 2007, 2010, in press) manipulation of neighboring bone pairs, to determine the best fit and the range of motion of each bone-bone articulation. Here, digital 3D data offers the great advantage of being weightless, so that even large numbers of bones can be articulated without the need for extensive support as exemplified by Senter and Robins (2005: fig. 1), and without the risk of damaging a specimen. Based on these data, the full mount can be created with minimal errors, as long as biomechanical implications of the overall posture such as bending moments and joint torque estimates are taken into account. Data on how the animals were found in the sediment can provide key pointers, and should always be used if available.

Reconstruction drawings are even more prone to errors than skeletal mounts, and errors are also harder to notice in drawings. As pointed out by Paul (2000), using second-hand data is not advisable. Especially important is the elimination of copying errors, caused by repeated re-drawing of skeletal elements. Here, modern computer technology also offers great advantages, allowing the error-free copying of elements in photo editing software, as used e.g., by Scott Hartman (www.skeletaldrawing.com; personal communication 2008).

Acknowledgements

The author thanks Hans-Ulrich Pfretzschner, Alexander Hohloch (both IFGT, Tübingen, Germany), Kristian Remes (Steinmann Institut, Universität Bonn, Bonn, Germany), Scott Hartmann (Wyoming Dinosaur Center, Thermopolis, USA) and Jonathan Rader (University of Wyoming, Laramie, USA) for helpful discussions. Rainer Schoch, Ronald Böttcher (both SMNS, Stuttgart, Germany) as well as Daniela Schwarz-Wings and Frieder Mayer (both MFN, Berlin, Germany) readily granted access to specimens in their care. Burkhard Ludescher (UHT, Tübingen, Germany) patiently scanned the entire skeleton of GPIT1. The manuscript has greatly benefitted from helpful reviews by Dewey Ray Wilhite (Auburn University College of Veterinary Medicine, Auburn, USA) and Andreas Christian (Universität Flensburg, Flensburg, Germany). This is contribution number 90 to DFG FOR 533 "Sauropod Biology".

References

Apesteguia, S. 2005. Evolution of the hyposphene-hypantrum complex within Sauropoda. *In*: V. Tidwell and K. Carpenter (eds.), *Thunder-Lizards: the Sauropodomorph Dinosaurs*, 258–267. Indiana University Press, Bloomington.

Bakker, R.T. 1986. *The Dinosaur Heresies*. 448 pp. William Morrow, New York.

Bonnan, M.F. 2003. The evolution of manus shape in sauropod dinosaurs: implications for functional morphology, forelimb orientation, and phylogeny. *Journal of Vertebrate Paleontology* 23: 595–613. http://dx.doi.org/10.1671/A1108

Bonnan, M.F. and Senter, P. 2007. Were the basal sauropodomorph dinosaurs *Plateosaurus* and *Massospondylus* habitual quadrupeds? *In*: P.M. Barrett and D.J. Batten (eds.), Evolution and Palaeobiology of Early Sauropodomorph Dinosaurs. *Special Papers in Palaeontology* 77: 139–155.

Bonnan, M.F., Sandrik, J., Nishiwaki, T., Wilhite, D., and Elsey, R. 2009. Calcified cartilage shape in extant archosaur long bones reflects overlying joint shape in load-bearing elements: implications for inferring dinosaur joint shape. *Journal of Vertebrate Paleontology* 29 (Supplement to No. 3): 67A–68A.

Carpenter, K. 2002. Forelimb biomechanics of nonavian theropod dinosaurs in predation. *Senckenbergiana Lethaea* 82: 59–76. http://dx.doi.org/10.1007/BF03043773

Carpenter, K. and Smith, M. 2001. Forelimb osteology and biomechanics of *Tyrannosaurus rex*. *In*: D.H. Tanke and K. Carpenter (eds.), *Mesozoic Vertebrate Life*, 90–116. Indiana University Press, Bloomington.

Christian, A. and Dzemski, G. 2007. Reconstruction of the cervical skeleton posture of *Brachiosaurus brancai* Janensch, 1914 by an analysis of the intervertebral stress along the neck and a comparison with the results of different approaches. *Fossil Record* 10: 38–49. http://dx.doi.org/10.1002/mmng.200600017

Christian, A. and Preuschoft, H. 1996. Deducing the body posture of extinct large vertebrates from the shape of the vertebral column. *Palaeontology* 39: 801–812.

Christian, A., Koberg, D., and Preuschoft, H. 1996. Shape of the pelvis and posture of the hind limbs in *Plateosaurus*. *Paläontologische Zeitschrift* 70: 591–601.

Claessens, L.P.A.M. 2009. The skeletal kinematics of lung ventilation in three basal bird taxa (Emu, Tinamou, and Guinea fowl). *Journal of Experimental Zoology* 309A: 14. http://dx.doi.org/10.1002/jrz.501

Cooper, M.R. 1981. The prosauropod dinosaur *Massospondylus carinatus* Owen from Zimbabwe: its biology, mode of life and phylogenetic significance. *Occasional Papers, National Museums and Monuments of Rhodesia, Series B, Natural Sciences* 6: 689–840.

Farmer, C.G. and Sanders, K. 2010. Unidirectional airflow in the lungs of alligators. *Science* 327: 338–340. http://dx.doi.org/10.1126/science.1180219

Fraas, E. and Berckhemer, F. 1926. *Führer durch die Naturaliensammlung zu Stuttgart I. Die Geognostische Sammlung Württembergs, zugleich ein Leitfaden für die geologischen Verhältnisse und zur Kenntnis der vorweltlichen Bewohner Württembergs. 5th edition*. 88 pp. Schweizerbart, Stuttgart.

Frappell, P.B., Hinds, D.S., and Boggs, D.F. 2001. *Physiological and Biochemical Zoology* 74: 75–89. http://dx.doi.org/10.1086/319300

Fujiwara, S.-I. 2009. A reevaluation of the manus structure in *Triceratops* (Ceratopsia: Ceratopsidae). *Journal of Vertebrate Paleontology* 29: 1136–1147. http://dx.doi.org/10.1671/039.029.0406

Galton, P.M. 1971a. Manus movements of the coelurosaurian dinosaur *Syntarsus rhodesiensis* and the opposability of the theropod hallux [sic]. *Arnoldia (Rhodesia)* 5: 1–8.

Galton, P.M. 1971b. The Prosauropod dinosaur *Ammosaurus*, the crocodile *Protosuchus*, and their bearing on the age of the Navajo Sandstone of Northeastern Arizona. *Journal of Paleontology* 45: 781–795.

Galton, P.M. 1976. Prosauropod dinosaurs of North America. *Postilla* 169: 1–98.

Galton, P.M. 1984. Cranial anatomy of the prosauropod dinosaur *Plateosaurus* from the Knollenmergel (Middle Keuper, Upper Triassic) of Germany. I. Two complete skulls from Trossingen/Württ. With comments on the diet. *Geologica et Palaeontologica* 18: 139–171.

Galton, P.M. 1985. Cranial anatomy of the prosauropod dinosaur *Plateosaurus* from the Knollenmergel (Middle Keuper, Upper Triassic) of Germany. II. All the cranial material and details of soft-part anatomy. *Geologica et Palaeontologica* 19: 119–159.

Galton, P.M. 1986a. Prosauropod dinosaur *Plateosaurus* (*Gresslyosaurus*) (Saurischia: Sauropodomorpha) from the Upper Triassic of Switzerland. *Geologica et Palaeontologica* 20: 167–183.

Galton, P.M. 1986b. Herbivorous adaptations of Late Triassic and Early Jurassic dinosaurs. *In*: K. Padian (ed.), *The Beginning of the Age of Dinosaurs*, 203–221. Cambridge University Press, Cambridge.

Galton, P.M. 1990. Basal Sauropodomorpha–Prosauropoda. *In*: D.B. Weishampel, P. Dodson, and H. Osmólska (eds.), *The Dinosauria*, 320–344. University of California Press, Berkeley.

Galton, P.M. 2000. The prosauropod dinosaur *Plateosaurus* Meyer, 1837 (Saurischia: Sauropodomorpha). I. The syntypes of *P. engelhardti* Meyer, 1837 (Upper Triassic, Germany), with notes on other European prosauropods with "distally straight" femora. *Neues Jahrbuch für Geologie und Paläontologie, Abhandlungen* 216: 233–275.

Galton, P.M. 2001. The prosauropod dinosaur *Plateosaurus* Meyer, 1837 (Saurischia: Sauropodomorpha; Upper Triassic). II. Notes on the referred species. *Revue Paléobiologie, Genève* 20: 435–502.

Graf, J., Stofft, E., Freese, U., and Niethard, F.U. 1993. The ultrastructure of articular cartilage of the chicken's knee joint. *International Orthopedics* 17: 113–119. http://dx.doi.org/10.1007/BF00183553

Gierlinski, G., Lockley, M., and Milner, A.R.C. 2005. Traces of Early Jurassic crouching dinosaurs. *In*: *Tracking Dinosaur Origins—The Triassic/Jurassic Terrestrial Transition, Abstract Volume*, 4. Dixie State College, St. George.

Gishlick, A.D. 2001. The function of the manus and forelimb of *Deinonychus antirrhopus* and its importance for the origin of avian flight. *In*: J. Gauthier and L.F. Gall (eds.), *New Perspectives on the Origin and Early Evolution of Birds*, 301–318. Yale Peabody Museum, New Haven.

Goslow, G.E. and Jenkins, F.A. 1983. The functional anatomy of the shoulder of the savannah monitor lizard (*Varanus exanthematicus*). *Journal of. Morphology* 175: 195–216. http://dx.doi.org/10.1002/jmor.1051750207

Gunga, H.-C., Suthau, T., Bellmann, A., Friedrich, A., Schwanebeck, T., Stoinski, S., Trippel, T., Kirsch, K., and Hellwich, O. 2007. Body mass estimations for *Plateosaurus engelhardti* using laser scanning and 3D reconstruction methods. *Naturwissenschaften* 94: 623–630. http://dx.doi.org/10.1007/s00114-007-0234-2

Gunga, H.-C., Suthau, T., Bellmann, A, Stoinski, S., Friedrich, A., Trippel, T., Kirsch, K., and Hellwich, O. 2008. A new body mass estimation of *Brachiosaurus brancai* Janensch 1914 mounted and exhibited at the Museum of Natural History (Berlin, Germany). *Fossil Record* 11: 28–33. http://dx.doi.org/10.1002/mmng.200700011

Henderson, D.M. 2006. Burly gaits: centers of mass, stability and the trackways of sauropod dinosaurs. *Journal of Vertebrate Paleontology* 26: 907–921. http://dx.doi.org/10.1671/0272-4634(2006)26%5B907:BGCOMS%5D2.0.CO;2

Hennig, E. 1915. *Kentrosaurus aethiopicus,* der Stegosauride des Tendaguru. *Sitzungsberichte der Gesellschaft naturforschender Freunde zu Berlin* 1915: 219–247.

Hirasawa, T. 2009. The ligamental scar in the costovertebral articulation of the tyrannosaurid dinosaurs. *Acta Palaeontologica Polonica* 54: 49–59. http://dx.doi.org/10.4202/app.2009.0106

Huene, F. von 1907–1908. Die Dinosaurier der europäischen Triasformation mit Berücksichtigung der aussereuropäischen Vorkommnisse. *Geologische und paläontologische Abhandlungen* I: 1–419.

Huene, F. von 1926. Vollständige Osteologie eines Plateosauriden aus dem schwäbischen Keuper. *Geologische und Palaeontologische Abhandlungen, Neue Folge* 15: 139–179.

Huene, F. von 1928. Lebensbild des Saurischer-Vorkommens im obersten Keuper von Trossingen in Württemberg *Palaeobiologica* 1: 103–116.

Huene, F. von 1932. Die fossile Reptil-Ordnung Saurischia, ihre Entwicklung und Geschichte. *Monographien zur Geologie und Paläontologie* 4: 1–361.

Jaekel, O. 1913–1914. Über die Wirbeltierfunde in der oberen Trias von Halberstadt. *Paläontologische Zeitschrift* 1: 155–215.

Landsmeer, J.M.F. *1983.* The mechanism of forearm rotation in *Varanus exanthematicus*. *Journal of Morphology* 175: 119–130. http://dx.doi.org/10.1002/jmor.1051750202

Landsmeer, J.M.F. 1984. Morphology of the anterior limb in relation to sprawling gait in *Varanus*. *Symposium of the Zoological Society of London* 52: 27–45.

Maina, J.N. and Nathaniel, C. 2001. A qualitative and quantitative study of the lung of an ostrich, *Struthio camelus*. *Journal of Experimental Biology* 204: 2313–2330.

Mallison, H. 2007. *Virtual dinosaurs-developing Computer Aided Design and Computer Aided Engineering modeling methods for vertebrate paleontology*. 102 pp. Unpublished Ph.D. thesis. Eberhard-Karls-Universität Tübingen, Tübingen. http://tobias-lib.ub.uni-tuebingen.de/volltexte/2007/2868/

Mallison, H. (in press). *Plateosaurus* in 3D—how CAD models and kinetic/dynamic modeling aid inbringing an extinct animal to life. *In*: N. Klein, K. Remes, C. Gee, and P.M. Sander (eds.), *Biology of the Sauropod Dinosaurs: Understanding the Life of Giants*. *Life of the Past* (series ed. J. Farlow). Indiana University Press, Bloomington.

Mallison, H. 2010. The digital *Plateosaurus* I: body mass, mass distribution, and posture assessed using CAD and CAE on a digitally mounted complete skeleton. *Palaeontologia Electronica*13 (2, 8A): 26.

Mallison, H., Hohloch, A., and Pfretzschner, H.-U. 2009. Mechanical digitizing for paleontology—new and improved techniques. *Palaeontologia Electronica* 12 (2, 4T): 41. http://palaeo-electronica.org/2009_2/185/index.html

Marsh, O.C. 1891. Restoration of *Triceratops*. *American Journal of Science* 41: 339–342.

doi:10.4202/app.2009.0075

Marsh, O.C. 1893a. Restoration of *Anchisaurus*. *American Journal of Science* 45: 169–170.

Marsh, O.C. 1893b. Restoration of *Anchisaurus*, *Ceratosaurus*, and *Claosaurus*. *Geological Magazine* 10: 150–157. http://dx.doi.org/10.1017/S0016756800170244

McGinnis, P.M. 2004. *Biomechanics of Sports and Exercise* (2nd ed.). 424 pp. Human Kinetics, Champaign.

Meyer, H. von 1837. Mitteilung an Prof. Bronn. *Neues Jahrbuch für Geologie und Paläontologie* 1837: 316.

Milner, A.R.C, Harris, J.D., Lockley, M.G., Kirkland, J.I., and Matthews, N.A. 2009. Bird-like anatomy, as posture, and behavior revealed by an Early Jurassic theropod dinosaur resting trace. *PloS One* 4 e4501 http://dx.doi.org/10.1371/journal.pone.0004591

Mortola, J.P. and Seguin, J. 2009. End-tidal CO_2 in some aquatic mammals of large size. *Zoology* 112: 77–85. http://dx.doi.org/10.1016/j.zool.2008.06.001

Moser, M. 2003. *Plateosaurus engelhardti* Meyer, 1837 (Dinosauria, Sauropodomorpha) aus dem Feuerletten (Mittelkeuper; Obertrias) von Bayern. *Zitteliana Reihe B* 24: 1–186.

O'Connor, P.M. and Claessens, L.P.A.M. 2005. Basic avian pulmonary design and flow-through ventilation in non-avian theropod dinosaurs. *Nature* 436: 253–256. http://dx.doi.org/10.1038/nature03716

Paul, G.S. 1987. The science and art of restoring the life appearance of dinosaurs and their relatives: a rigorous how-to guide. *In*: S.J. Czerkas and E.C. Olson (eds.), *Dinosauria Past and Present, Vol. 2*, 5–49. University of Washington Press, Seattle.

Paul, G.S. 1996. *The Complete Illustrated Guide to Dinosaur Skeletons*. 97 pp. Gakken Mook, Japan.

Paul, G.S. 1997. Dinosaur models: the good, the bad, and using them to estimate the mass of dinosaurs. *In*: D.L. Wolberg, E. Stump, and G. Rosenberg (eds.), *Dinofest International: Proceedings of a Symposium Held at Arizona State University*, 129–154. Academy of Natural Sciences, Philadelphia.

Paul, G.S. 2000. Restoring the life appearance of dinosaurs. *In*: G.S. Paul (ed.), *The Scientific American Book of Dinosaurs*, 78–106. Byron Press and Scientific American, New York.

Paul, G.S. 2005. Body and tail posture in theropod dinosaurs. *In*: K. Carpenter (ed.), T*he Carnivorous Dinosaurs*, 238–246. Indiana University Press, Bloomington.

Paul, G.S. 2008. A revised taxonomy of the iguanodont dinosaur genera and species. *Cretaceous Research* 29: 192–216. http://dx.doi.org/10.1016/j.cretres.2007.04.009

Perry, S.F. 2001. Functional morphology of the reptilian and avian respiratory systems and its implications for theropod dinosaurs. *In*: J. Gauthier J. and L.F. Gall (eds.), *New Perspectives on the Origin and Early Evolution of Birds. Proceedings of the International Symposium in Honor of John H. Ostrom*, 429–442. Special Publication of the Peabody Museum of Natural History, Yale University, New Haven.

Remes, K. 2008. Evolution of the pectoral girdle and forelimb in Sauropodomorpha (Dinosauria, Saurischia): Osteology, myology and function. 352 pp. Unpublished Ph.D. thesis, Ludwig-Maximilians Universität, München. http://edoc.ub.uni-muenchen.de/8395/

Sander, P.M. 1992. The Norian *Plateosaurus* bonebeds of central Europe and their taphonomy. *Palaeogeography, Palaeoclimatology, Palaeoecology* 93: 255–299. http://dx.doi.org/10.1016/0031-0182(92)90100-J

Senter, P. 2006a. Comparison of forelimb function between *Deinonychus* and *Bambiraptor* (Theropoda: Dromaeosauridae). *Journal of Vertebrate Paleontology* 26: 897–906. http://dx.doi.org/10.1671/0272-4634(2006)26%5B897:COFFBD%5D2.0.CO;2

Senter, P. 2006b. Forelimb function in *Ornitholestes hermanni* Osborn (Dinosauria, Theropoda). *Palaeontology* 49: 1029–1034. http://dx.doi.org/10.1111/j.1475-4983.2006.00585.x

Senter, P. and Parrish, J.M. 2006. Forelimb function in the theropod dinosaur *Carnotaurus sastrei*, and its behavioral implications. *PaleoBios* 26: 7–17.

Senter, P. and Robins, J.H. 2005. Range of motion in the forelimb of the theropod dinosaur *Acrocanthosaurus atokensis*, and implications for predatory behaviour. *Journal of Zoology* 266: 307–318. http://dx.doi.org/10.1017/S0952836905006989

Stahl W.R. 1967. Scaling of respiratory variables in mammals. *Journal of Applied Physiology* 22: 453–460.

Stevens, K.A. and Parrish, J.M. 1999. Neck posture and feeding habits of two Jurassic sauropods. *Science* 284: 798–800.

Stevens, K.A. and Parrish, J.M. 2005a. Digital reconstructions of sauropod dinosaurs and implications for feeding. *In*: K.A. Curry-Rogers and J.A. Wilson (eds.), *The Sauropods: Evolution and Paleobiology*, 178–200. University of California Press, Berkeley. http://dx.doi.org/10.1126/science.284.5415.798

Stevens, K.A. and Parrish, J.M. 2005b. Neck posture, dentition, and feeding strategies in Jurassic sauropod dinosaurs. *In*: K. Carpenter and V. Tidwell (eds.), *Thunder Lizards: The Sauropodomorph Dinosaurs*, 212–232. Indiana University Press, Bloomington.

Stevens, K.A., Larson, P., Wills, E.D., and Anderson, A. 2008. Rex, sit: Digital modeling of *Tyrannosaurus rex* at rest. *In*: P. Larson and K. Carpenter (eds.), Tyrannosaurus rex*, the Tyrant King*, 193–204. Indiana University Press, Bloomington.

Taylor, M.P., Wedel, M.J., and Naish, D. 2009. Head and neck posture in sauropod dinosaurs inferred from extant animals. *Acta Palaeontologica Polonica* 54: 213–220. http://dx.doi.org/10.4202/app.2009.0007

Therrien, F. and Henderson, D.M. 2007. My theropod is bigger than yours… or not: Estimating body size from skull length in theropods. *Journal of Vertebrate Paleontology* 27: 108–115. http://dx.doi.org/10.1671/0272-4634(2007)27%5B108:MTIBTY%5D2.0.CO;2

Weems, R.E. 2003. *Plateosaurus* foot structure suggests a single trackmaker for *Eubrontes* and *Gigandipus* footprints. *In*: P.M. LeTourneau and P.E. Olsen (eds.), *The Great Rift Valleys of Pangea in Eastern North America, Vol. 2: Sedimentology, Stratigraphy, and Paleontology*, 293–313. Columbia University Press, New York.

Wedel, M.J. 2003. Vertebral pneumaticity, air sacs, and the physiology of sauropod dinosaurs. *Paleobiology* 29: 243–255. http://dx.doi.org/10.1666/0094-8373(2003)029%3C0243:VPASAT%3E2.0.CO;2

Wedel, M.J. 2007. What pneumaticity tells us about "prosauropods" and vice versa. *In*: P.M. Barrett and D.J. Batten (eds.), Evolution and Palaeobiology of Early Sauropodomorph Dinosaurs. *Special Papers in Palaeontology* 77: 207–222.

Wedel, M.J. 2009. Evidence for bird-like air sacs in saurischian dinosaurs. *Journal of Experimental Zoology* 311A: 1–18. http://dx.doi.org/10.1002/jez.513

Weishampel, D.B. and Westphal, F. 1986. *Die Plateosaurier von Trossingen*. 27 pp. Attempto, Tübingen.

Wellnhofer, P. 1994. Prosauropod dinosaurs from the Feuerletten (Middle Norian) of Ellingen near Weissenburg in Bavaria. *Revue de Paleobiologie, Volume spécial* 7 (1993): 263–271.

Wilson, J.A. 1999. A nomenclature for vertebral laminae in sauropods and other saurischian dinosaurs. *Journal of Vertebrate Paleontology* 19: 639–653.

Witmer, L.M. 1995. The extant phylogenetic bracket and the importance of reconstructing soft tissues in fossils. *In*: J.J. Thomason (ed.), *Functional Morphology in Vertebrate Paleontology*, 19–33. Cambridge University Press, New York.

Yates, A.M. 2003. The species taxonomy of the sauropodomorph dinosaurs from the Löwenstein Formation (Norian, Late Triassic) of Germany. *Palaeontology* 46: 317–337. http://dx.doi.org/10.1111/j.0031-0239.2003.00301.x

Yates, A.M. and Vasconcelos, C.C. 2005. Furcula-like clavicles in the prosauropod dinosaur *Massospondylus*. *Journal of Vertebrate Paleontology* 25: 466–468. http://dx.doi.org/10.1671/0272-4634(2005)025%5B0466:FCITPD%5D2.0.CO;2

Ziegler, B. 1988. Führer durch das Museum am Löwentor. *Stuttgarter Beiträge zur Naturkunde, Series C* 27E: 1–100.